1972

A mass spectrometric characterization of positive ions created in simple vacuum diodes incorporating oxide cathodes with supplementary analysis of background gases

Larry A. Addington

Department:

A MASS SPECTROMETRIC CHARACTERIZATION OF POSITIVE IONS CREATED IN SIMPLE VACUUM DIODES INCORPORATING OXIDE CATHODES WITH SUPPLEMENTARY ANALYSIS OF BACKGROUND GASES

BY

LARRY ALTON ADDINGTON, 1947-

A THESIS

Presented to the Faculty of the Graduate School of the

UNIVERSITY OF MISSOURI-ROLLA

In Partial Fulfillment of the Requirements for the Degree

MASTER OF SCIENCE IN CERAMIC ENGINEERING

1972

Approved by

_____ (Advisor) _____

_____

ABSTRACT

Simple diodes were constructed utilizing oxide cathodes and nickel anodes. The cathodes were obtained by applying a mixture of barium, strontium, and calcium carbonates to a nickel filament and decomposing them to yield the oxides. The products of decomposition were analyzed by monitoring the composition of the background gases in the vacuum chamber.

A portion of the flux of positive ions bombarding the cathode during diode operation was analyzed. It was possible to determine the region of origin of the ions and their potential energy at the time of formation. Positive ions of chlorine, fluorine, sodium, potassium, and rubidium were released at the anode surface when an emission current was drawn. The relative heights of the peaks due to ions created in the interelectrode space were very sensitive to processes occurring in the diode region. Changes in the shape of the peaks due to ions created in the interelectrode space were related to changes in the activity of the cathode and the amount of space charge surrounding the cathode.

The transport of BaO was observed in the mass spectra taken at a cathode temperature of 1370°C. Nondispersive x-ray analysis of the anode facing the cathode operated at 1370°C revealed the presence of barium and strontium.

ACKNOWLEDGEMENTS

The author wishes to acknowledge Dr. Gordon Lewis, his advisor, for his assistance throughout the research and Drs. P. D. Ownby and Leonard Levenson for their suggestions concerning the writing of the thesis. The author acknowledges the Western Electric Company for supplying the carbonate mix and the accompanying information and the Somers Thin Strip Company for supplying the cathode nickel and its analysis. The author also acknowledges the Graduate Center for Materials Research, University of Missouri-Rolla, and the National Science Foundation for their support of this research. The author acknowledges his wife, Janet, for her encouragement and patience during the research and the writing of this thesis.

TABLE OF CONTENTS

LIST OF ILLUSTRATIONS

Figures Page

LIST OF TABLES

I. INTRODUCTION

The oxide cathode began to be utilized as an electron emitter in vacuum devices soon after its discovery in 1904. It became the standard cathode in the electron tube industry. During the past two decades solid state devices have replaced electron tubes in many applications; however, the oxide cathode is still of great importance. Two of the more common modern electron devices using the oxide cathode are cathode ray tubes and high power microwave transmission tubes.

The residual gas atmosphere in which the cathode operates is closely related to the state of the cathode and its emissive properties.[1] Various studies[1,2,3,4] have been conducted to relate the manufacturing process and the resulting cathode properties to the gaseous phase. Some of these studies were conducted using mass spectrometric analysis of changes in composition of the gas in a processing chamber during the significant stages of processing and operation. The mass spectrometer was used to determine the composition of the gaseous phase[3,4] and to investigate the emission of negative ions from the cathode surface.[5,6,7,8]

During normal operation of an electron tube, gas molecules are ionized by electron emission and are accelerated toward the cathode due to the field applied by the plate voltage (V_p). This is referred to as positive ion bombard-

ment, and it is an important mode of interaction between the cathode and the gaseous phase. Changes in the emissive properties of the cathode produced by positive ion bombardment have been investigated,[9] but attention was not focused on the ions themselves.

The first objective of the present investigation was to use the mass spectrometer to observe directly the ions created within the interelectrode space. In addition to ascertaining the masses of these ions, and hence identifying them, it was also possible to determine their region of origin and approximate potential energy with reference to the cathode or anode at the time of formation. The second objective was to analyze the background composition of the gaseous phase within the sample chamber during cathode processing and operation.

II. REVIEW OF LITERATURE ON THE OXIDE CATHODE

A. A Brief Survey of the Cathode Development

The electron emitting properties of the alkaline earth oxides were first studied in 1904, when Wehnelt investigated the unusually high emission of CaO on platinum filaments.[10] Shortly thereafter, the emitting properties of other alkaline earth oxides, particularly BaO and SrO, were studied. The obtainable emission currents for well activated cathodes were found to decrease in the following order: BaO, SrO, and CaO.[1] Mixtures of the oxides of Ba and Sr were studied by Benjamin and Rooksby[2] and they found the highest emission currents were obtained for filaments coated with a 54% SrO and 46% BaO mixture by weight.[2]

The alkaline earth oxides are unstable under ambient atmospheric conditions, because they convert to hydroxides and carbonates. In order to obtain a well characterized coating material and facilitate handling, alkaline earth carbonates rather than oxides, are applied to the filament. The material which is applied to the filament consists of the carbonates and a suitable binder, such as nitrocellulose, in a vehicle such as amyl acetate. The carbonates are decomposed to yield the oxides during the early stages of processing.[11] The decomposition will be discussed in more detail in a later section.

The core metal from which the filament is made must have

a relatively low vapor pressure and should have a favorable influence on emission. Some metals having a sufficiently low vapor pressure at the operating temperature of the cathode are nickel, platinum, molybdenum, tantalum, and tungsten. Of these, nickel seems to be most favorable to emission and is most often used.[11] Small additions of alloying agents are added to the nickel to produce cathodes of even higher activity.

B. The Physics of the Oxide Cathode

1. Electronic Structure

The physical and chemical nature of the oxide cathode has been a subject of intense interest to investigators; however, a unified theory which accounts for the major peculiarities of the cathode has been developed only in the past two or three decades.[12] Advances in semiconductor theory made during that time were of prime importance to the development of the theory.

Early investigators correlated active cathodes with reducing conditions. Becker[13] found that excess barium was formed in and evolved by a [BaSr]O* cathode at 987°C by observing its effect on the emission of a facing tungsten ribbon. Quantitative measurements of the excess barium concentration in cathodes made from barium, strontium,

---

*[BaSr]O designates a mixed oxide coating consisting of a solid solution between BaO and SrO.

and nickelous carbonates were made by Prescott and Morrison[14] in 1938. Similar determinations were made by others.[1] The average value of the excess barium concentration was found to be about 5×10^{-2} mole percent.

The effectiveness of an adsorbed layer of an electropositive element in lowering the work function and increasing the emission of metallic filaments was well known at that time[15] and the extension to the oxide cathode seemed obvious. Calculations showed, however, that the accommodation of this amount of barium on the surface of the cathode would require a coverage of approximately 100 monolayers,[1] which would lead to a bulk type behavior characteristic of metallic barium. This was not the case since the vapor pressure of metallic barium at the operating temperatures of the oxide cathode is about 1 mm,[16] which is much higher than that observed. It is obvious that much of the excess barium must be found within the crystal lattice of the oxide material, as atomic defects.

Photoconductivity[17] and photoelectrical[18] studies of BaO indicated the existence of donors lying 1.4 eV and 2.3 eV below the conduction band with a total band gap of 3.8 eV. These findings are summarized by Krumhansl.[19] Interstitial barium atoms or oxygen vacancies could act as donors; however, diffusion studies summarized by Thomas[18] favor oxygen vacancies. Hall coefficient experiments were later performed by Pell[20] and indicated negative charge

carriers which further supported the existence of donors.

The oxide cathode is presently viewed as an n-type semiconductor in contact with a metal base. The electronic structure (in the absence of an applied field) is shown in Figure 1.[12]

2. Emission

At high cathode temperatures or low anode voltages electrons are emitted by the cathode at a faster rate than they can be swept away by the applied field. In this case an electron cloud is formed in front of the cathode creating a barrier to further emission. The amount of existing space charge is determined by an equilibrium between the rate at which electrons leave the cathode surface and the rate at which they return from the space charge region.[21] The amount of existing space charge is therefore determined by the activity of the cathode, the cathode temperature, and the anode voltage.

If the above parameters are manipulated in the proper manner the space charge can be reduced and finally removed. By carefully controlling the parameters, the applied field at the cathode surface may be maintained at zero. A theoretical treatment by Schottky of the zero field thermionic emission from an excess semiconductor, the electronic structure of which is shown in Figure 1, resulted in a Richardson type relationship. This relationship is given by equation (1).[22]

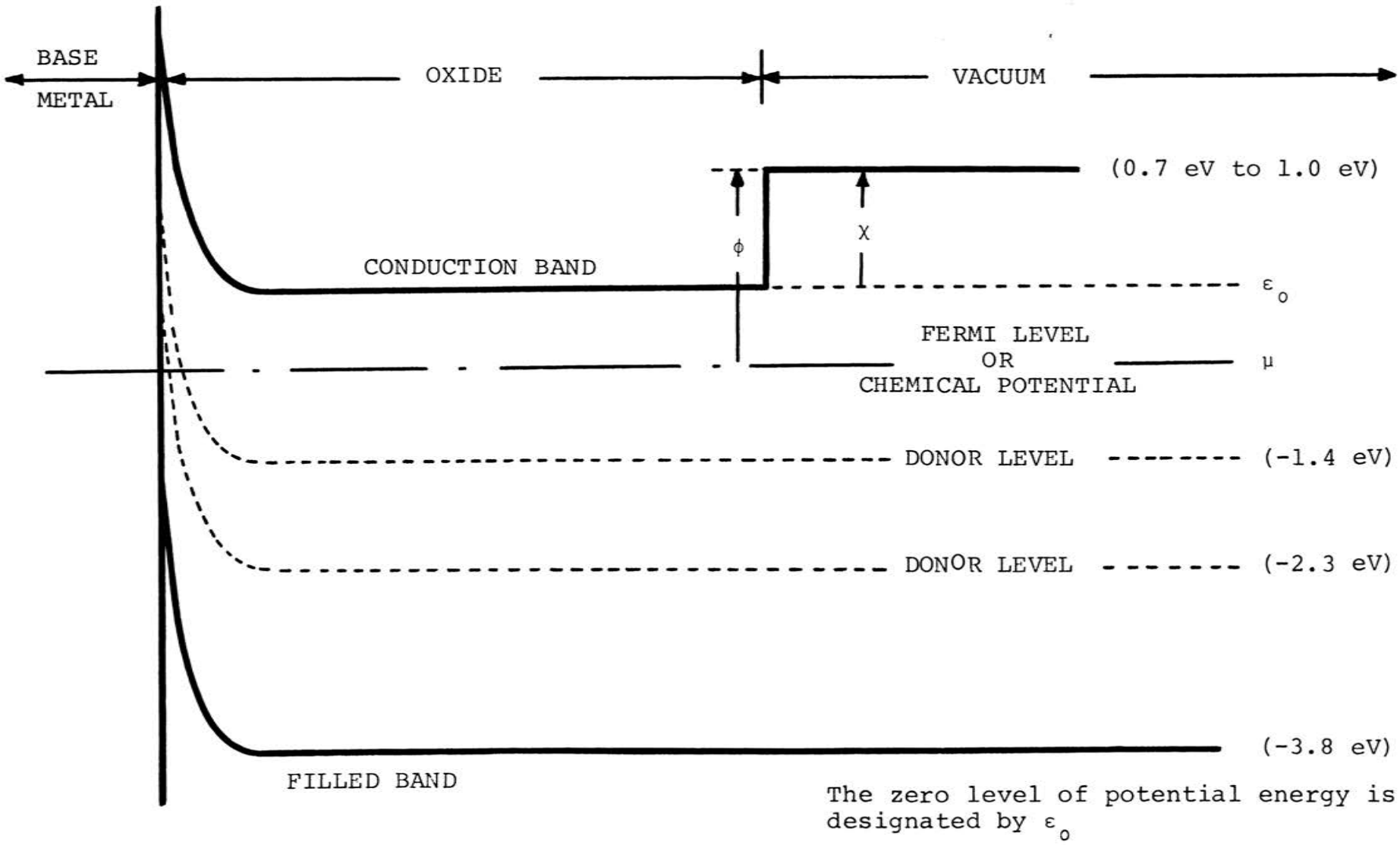

Figure 1. The Energy Level Structure of BaO

$$j_o = A\ (1-r)\ T^2 \exp\left[-\frac{e\ \phi}{k\ T}\right] \qquad (1)$$

Where: j_o = the zero field current density

A = the thermionic emission constant

r = the mean reflection coefficient for electrons at the emitting surface

T = the temperature in °K

k = the Boltzmann constant

e = the electronic charge

ϕ = the total work function

The total work function, ϕ, is the difference between the potential energy of the Fermi level and the potential energy of the vacuum level outside the crystal and is given by equation (2).

$$\phi = \chi + \varepsilon_o - \mu \qquad (2)$$

Where: χ = the electron affinity or external work function

ε_o = the zero level of potential energy

μ = the Fermi level or chemical potential (also called the internal work function)

As the concentration of donors increases the Fermi level is raised and the total work function is decreased as shown by equation (2). This yields an increase in emission as shown by equation (1). The importance of excess barium to the activity of the cathode is thus established by modern semiconductor theory.

If a cathode is operating in a zero field condition and the anode voltage is increased, with cathode temperature and activity remaining constant, the emission current will be increased due to a lowering of the external work function by the applied field. This phenomenon is known as the Sckottky effect.[23] The emission equation formulated by Schottky that applies in this region is given by equation (3).[1]

$$\log j_s = \log j_o + \frac{6.0}{T\sqrt{d}}\sqrt{V_p} \qquad (3)$$

Where: j_s = the saturated emission current density

j_o = the zero field emission current density

T = the temperature in °K

d = the cathode to anode distance

V_p = the anode voltage

A plot of log j_s vs $\sqrt{V_p}$ can be used to separate the space charge region of operation from the Schottky region. Ideally, a plot of the type shown in Figure 2 [1] would be obtained. A linear relationship should hold in the Schottky region. The deviation from linearity separates the space charge region from the Schottky region.

Plots of this type often show marked deviations from the ideal shape due to changes in cathode temperature or activity while the data are being taken. Perfectly plane cathode and anode surfaces were assumed to exist in the derivation of equation (3) and deviations from this assumption in real cathodes and anodes disturb the results.[1]

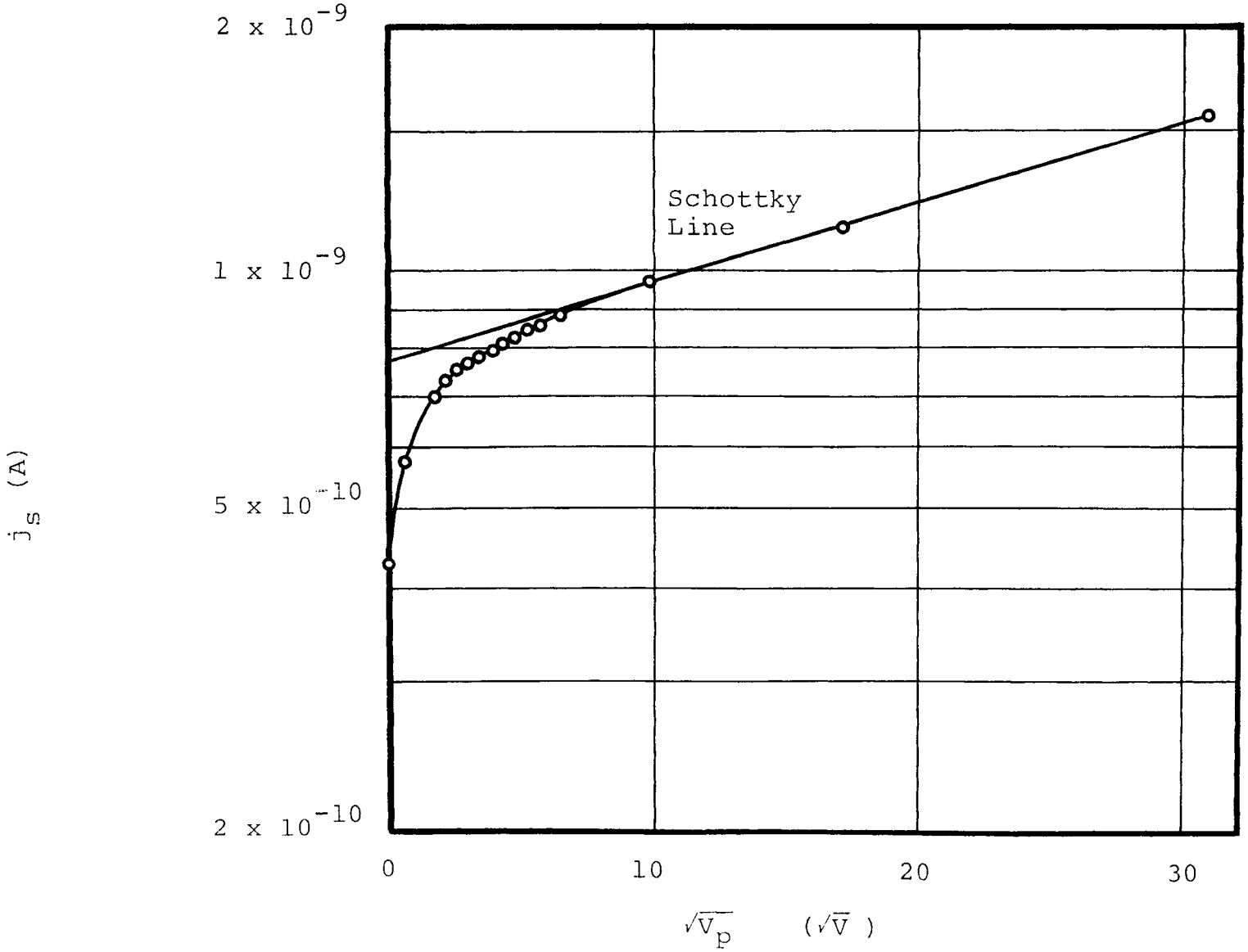

Figure 2. A Schottky Type Plot of Cathode Emission

C. Processing and Operating the Oxide Cathode

1. Decomposition and Activation

After the alkaline earth carbonates are applied they must be decomposed to yield the oxides according to the following reaction.

$$BaCO_3(s) \rightleftarrows BaO(s) + CO_2(g) \qquad (4)$$

The maximum rate of conversion from carbonate to oxide occurs between 900°C and 1100°C.[24]

The reduction of the oxide coating is referred to as the activation procedure and it is carried out immediately following the conversion. The most effective alloying agents or "activators" are elements, dissolved in the nickel, which are able to react with the coating according to the following reaction and yield an equilibrium pressure of Ba(g) which is calculated to equal the equilibrium pressure of barium metal at the temperature under consideration.[25]

$$BaO(s) + M(alloy) \rightleftarrows MO(s) + Ba(g) \qquad (5)$$

The metals having oxides with sufficiently large heats of formation to yield the limiting pressure of Ba at 727°C are: Al, Be, Hf, La, Mg, Nd, Pr, Sc, Si, Sm, Th, U, Y, and Zr. The additions are normally held under 1%. Not all of the elements listed are suitable for use as activators since they may yield barium compounds

which act as barriers to further diffusion.[25] In addition, these compounds may possess high electrical resistivities and lead to low cathode conductivity. This has been observed with Si.[12]

Another reaction that may proceed simultaneously with the decomposition reaction occurs between the barium carbonate and the activators.[25] A similar reaction may occur between the barium carbonate and any carbon remaining in the coating after the binder is decomposed at about 450°C to 500°C.[25] This reaction proceeds as follows:

$$BaCO_3(s) + M(alloy) \rightleftarrows BaO(s) + MO(s) + CO(g) \qquad (6)$$

It is apparent that this reaction competes with the reaction of equation (5) for the activator and leads to lower cathode activities than would otherwise be obtained.

Any gaseous reductants within the tube would be able to produce an activating effect by reducing the oxide coating if present at a sufficiently high partial pressure. Rittner[25] calculates that CO and H_2 would be moderately active reducing agents at a pressure of one atmosphere.

Applying an anode potential and drawing an emission current is observed to aid in activation.[1] The excess barium is thought to be produced by an electrolytic dissociation of the barium and oxygen ions in the lattice with expulsion of the electronegative oxygen at the surface.

It is important that barium be supplied at a sufficiently high activity that the oxide lattice may absorb it by diffusion in a reasonable period of time. It is desirable to complete the activation process as quickly as possible in industry for economic reasons.

2. Changes in Cathode Activity

The activity of the oxide cathode is determined by a complex interaction of temperature, stoichiometry, residual gas composition, and the emission current being drawn. The reaction of the cathode to contamination or poisoning is well known.[1,9] Investigators have found that an increase in oxygen partial pressure always leads to poisoning. At low cathode temperatures or high oxygen partial pressures the drop in emission is permanent and can be restored only by "reactivation" at a higher temperature. At high cathode temperatures or low oxygen partial pressure the emission returns to its former value when the oxygen is pumped off.[1]

Carbon dioxide and carbon monoxide tend to decrease emission at higher temperatures and increase emission at lower temperatures. Chlorine and water vapor have also been shown to cause poisoning.[1]

Heating the cathode to temperatures significantly above the operating temperature or "flashing" has been found to deactivate the cathode. Benjamin and Rooksby[2]

found that repeated flashing at 1327°C increased the emission current measured at 747°C after the first ten flashes. The emission current measured after each subsequent flash decreased until the emission was destroyed after twenty-one flashes and could not be restored.

D. Mass Spectrometric Investigations

The investigations in which the mass spectrometer has been used can generally be classified as the determination of the products of decomposition and activation, the observation of ions originating at the cathode surface, or the examination of the ions obtained when anodes were subjected to electron bombardment.

1. Products of Decomposition and Activation

This type of study has been undertaken by Thibault and Secretin[3] and Stier.[4] All of these investigators report the appearance of large peaks in the spectrum of the background gasses at masses 28 and 44. These peaks were attributed to CO^+ and CO_2^+ respectively. The mass spectrum of CO_2 exhibits peaks at both of these masses* due to fragmentation of the CO_2 molecule by the ionizing

---

* The masses of the most abundant CO and CO_2 molecules are actually 28.0038 amu and 44.0038 amu respectively. In this research the small deviations from integral mass values need not be considered, and mass numbers will be used to differentiate among ionic species. The mass number of a species is equal to the number of nucleons which it contains.

beam of the mass spectrometer. When the spectra of pure CO_2 and the products of decomposition were compared, the relative height of the mass 28 peak was larger in the latter than could be explained by the fragmentation of CO_2. Thibault and Secretin[3] believed that reduction of CO_2 by alkali metals they found emitted from bare nickel filaments was responsible for the excess height of the mass number 28 peak. They also thought the organic fragment $C_2H_4^+$ contributed to this peak. They observed a simultaneous increase in the mass number 27 peak which they attributed to $C_2H_3^+$. Both of the latter were believed to be products of decomposition of the nitrocellulose binder contained in the carbonate paste. Stier[4] attributed the excess height of the mass number 28 peak to the reduction of BaO by carbon contained in the coating as a result of binder decomposition. This would proceed as shown by equation (5); however, carbon would be the reducing agent and CO(g) would be formed rather than MO(s).

The mass spectrometer was used by Plumlee and Smith[26] to monitor changes in the background gas composition when an emission current was drawn on an oxide cathode. Their data showed an increase in the molecular oxygen peak (mass number 32) as the emission current was increased.

2. Analysis of Ions Emitted by the Cathode

Investigations of ions originating at the cathode surface have included searches for both positive and negative

ions. The emission of positive ions of the alkali metals from heated nickel filaments was observed by Thibault and Secretin[3] and by Plumlee and Smith.[26] Oxide coated filaments were not observed to emit alkali ions. Thibault and Secretin believed that in the latter case alkalis originating on the nickel filament were consumed in reducing part of the CO_2 remaining at the cathode surface after decomposition. CO would be produced by such a reduction. This was the basis for their interpretation of the excess height of the CO^+ peak which was discussed in the preceding section.

A number of studies have been conducted on the emission of negative ions from oxide cathodes.[3,5-8,26,27] The investigators report the observation of negative ions of mass numbers 12, 16, 26 , 27, 32, 35, 37 , 42, 43, and 44. Only those of mass numbers 16, 35, and 37 are of any stability or duration. Mass number 16 was attributed to O^- and mass numbers 35 and 37 to Cl^-. The experiments indicate that chlorine is emitted by the cathode as a negative ion,[5] while oxygen is released in the atomic state and subsequently converted to a negative ion.[6]

Plumlee and Smith[26] have proposed three mechanisms by which negative ions can be formed in partially evacuated systems. These are: (1) thermal evaporation from surfaces, (2) conversion of positive ions to negative ions upon striking a surface, (3) positive ion impact causing the dislodging of adsorbed materials as negative ions. The

ions formed in cases (2) and (3) may possess excess kinetic energy.

3. Analysis of Ions Produced by Electron Bombardment

Young[28] observed the release of Cl^+ ions during initial bombardment of anodes of silver, copper, nickel , molybdenum, tantalum, titanium, and tungsten. The Cl^+ peaks were strong just after outgassing the cathode, but decayed after a few hours. He thought cathode outgassing was the ultimate source of the chlorine. Young also observed the release of O^+ ions from previously oxidized anodes of copper, nickel, molybdenum, tantalum, and titanium when subjected to electron bombardment by 90 eV electrons at 10 mA/cm^2. The intensity of the O^+ peak was reduced to a small value by outgassing the anode with an internal heater.

Plumlee and Smith[26] observed the ejection of O^+ ions from hydrogen fired Mo anodes at anode temperatures above 300°C after briefly heating to 900°C indicating that residual gases reacted with the metal surface or impurities diffused to the surface to provide the source of oxygen. At anode temperatures above 850°C Na^+ and K^+ ions were created at or near the anode during electron bombardment. Plumlee and Smith also observed the ejection of Cl^+ ions from hydrogen fired copper.

III. EXPERIMENTAL

A. Equipment

The principal research instrument used in this investigation was a 30.5 cm (12 in.) radius, 90° magnetic sector, single focusing, high temperature mass spectrometer, manufactured by the Nuclide Corporation. The mass spectrometer was of stainless steel construction with the exception of the glass envelope of the Bayard-Alpert type ionization gauge. The gauge was located on a 1.8 cm i.d. appendage 16 cm in length which was attached to the system between the sample chamber of the mass spectrometer and its pump. Pumping was provided by two 7.62 cm (3 in.) three stage mercury diffusion pumps with separate thermoelectrically cooled baffles and liquid nitrogen vapor traps. One pump was employed in pumping the analyzer section of the mass spectrometer and the other was employed in pumping the sample chamber. The sample chamber was cylindrical with an i.d. of 14.9 cm and a volume of approximately 3 liters. The forevacuum was maintained by a Welch rotary oil vacuum pump. Pressures of 3.0×10^{-7} Torr were obtained without baking the system.

An experimental diode was designed to meet the constraints imposed by the experimental conditions and the objectives of the research. The diode was placed in the sample chamber and used in conjunction with the instrument's

standard ion source in order to accomplish both of the previously discussed objectives. The analysis of the overall composition of the gaseous phase within the sample chamber was used to determine the products of decomposition of the carbonate coating and to study the spectrum of pure CO_2. The other mode of operation was the direct observation of the ions created within the interelectrode space. From this data the region of origin and approximate potential energy of the ions at the time of formation were determined.

The analysis of the overall composition of the gaseous phase within the sample chamber was performed on ions created in the mass spectrometer's standard ion source. The sample chamber and ion source are shown in Figure 3. Electrons supplied by a hot tungsten filament were accelerated through a potential, variable from 0 to 100 v. The ion source accelerating potential was variable from 0 to 5 kV positive with respect to ground. The ions were normally created at a potential of 2.5 kV by collision with electrons having an energy of 70 eV. The ions were created within a nearly equipotential region before being focused and accelerated through the source plates.

Figure 3 illustrates the design and placement of the experimental diode. The cathode, on one side, faced the ion source of the mass spectrometer at a distance of 3.5 cm. The other side of the cathode faced the anode of the

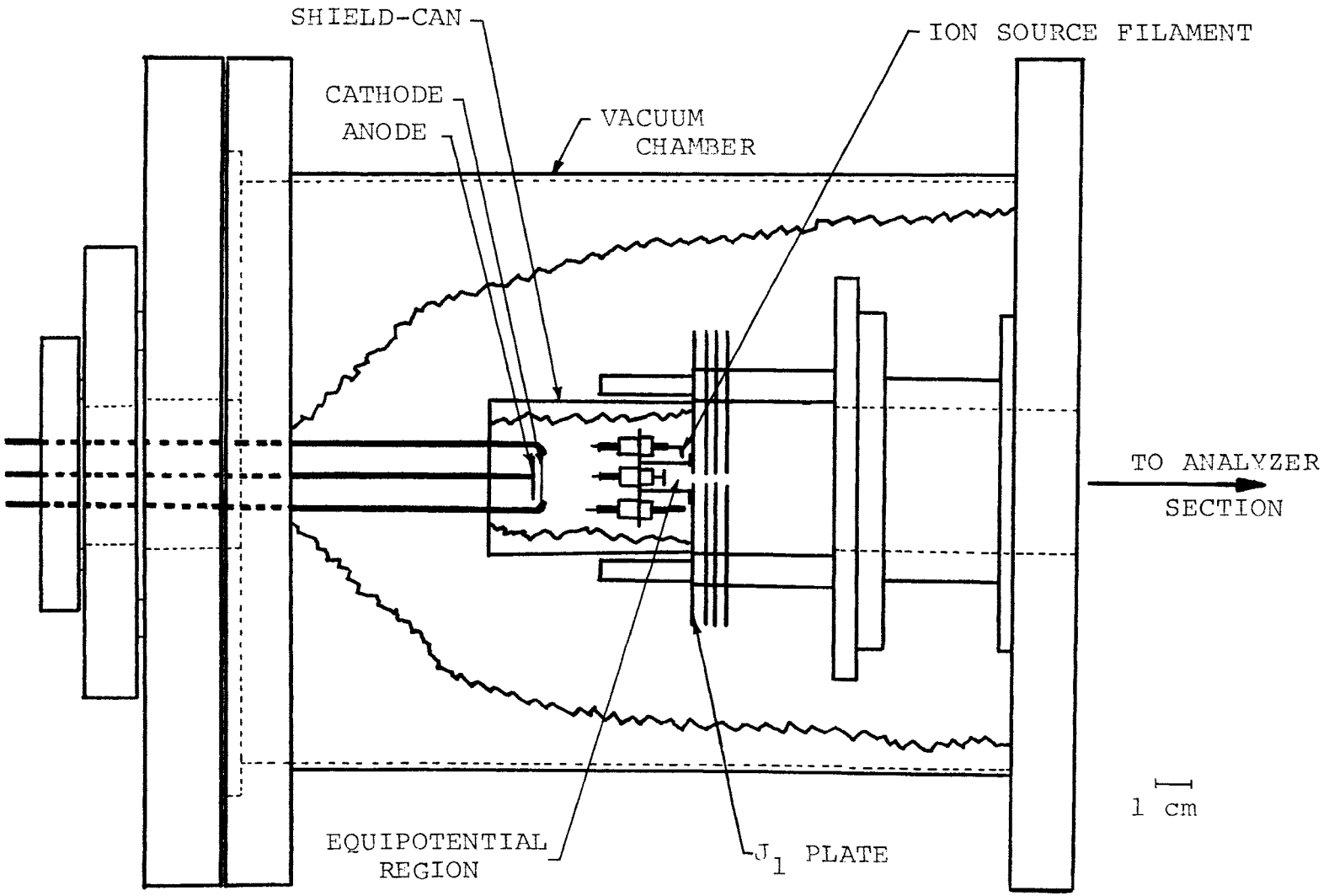

Figure 3. The Relationship Between the Experimental Diode and the Mass Spectrometer Ion Source

experimental diode. The cathode-to-anode spacing was 0.164 cm.

The objective of analyzing the ions produced by the experimental diode was achieved in the following manner. The filament that supplied ionizing electrons for the mass spectrometer ion source was turned off. This allowed the ions created by the experimental diode to be analyzed without interference due to additional ionization occurring in the ion source. It was necessary to provide the proper potential gradient from the anode of the experimental diode to the analyzer section of the mass spectrometer. The only change made in the ion source was to turn the filament off; therefore, the ions created by the diode were focused and accelerated by the source upon reaching its first accelerating plate. This was designated the J_1 plate. The cathode was set at a potential V_{jc} volts more positive than that of the J_1 plate, and the anode was set at a potential V_p volts more positive than that of the cathode. This provided the gradient required to accelerate the positive ions to the J_1 plate. The experimental arrangement used to achieve the potential gradient is shown schematically in Figure 4. The voltages V_{jc} and V_p were supplied by surplus U.S. Army power supplies PP-351/U-B2 and PP-351/U-B1 respectively. Both power supplies provided regulated dc voltage variable from 12.5 V to 150 V.

The ions, whether created by the experimental diode or by the mass spectrometer ion source, were accelerated by

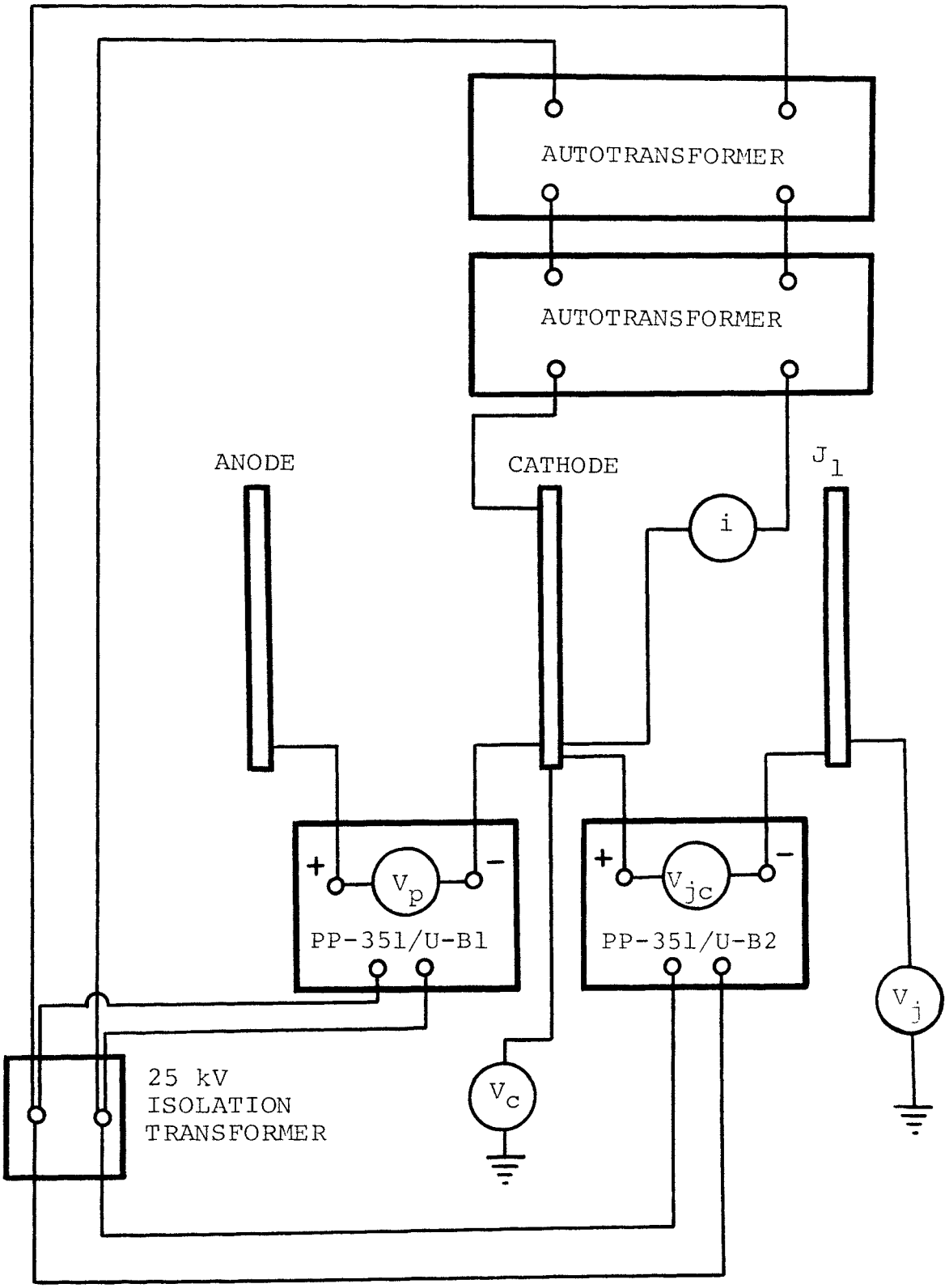

Figure 4. Equipment Establishing the Potential Gradient for Accelerating Ions Created in the Experimental Diode.

the source and directed through the magnetic field of the analyzer section for mass discrimination. After mass discrimination the ion current was amplified by a sixteen stage electron multiplier. The output of the multiplier went to an electrometer amplifier which was used to drive either a strip chart recorder or an oscillographic recorder.

The cathode was directly heated by 60 cycle ac power, using two autotransformers in series as shown in Figure 4. The uncoated filament dimensions were 0.005±0.0003 cm x 0.061±0.003 cm x 1.1±0.1 cm, and the anode dimensions were approximately 0.02 cm x 0.39 cm x 1.27 cm. The filament and anode were spot welded to support leads made from 0.152 cm diameter copper-cored stainless steel wire.

A gas inlet system was fabricated from 0.636 cm (1/4 in.) o.d. copper tubing. Nupro B-4H brass body bellows valves controlled the gas flow. A separate rotary oil vacuum pump was used to rough the inlet system. This system allowed pure gases of known composition to be admitted into the sample chamber which facilitated the interpretation of other data.

A Japan Electron Optics Laboratory Company model JSM-2 scanning electron microscope was used to investigate a black, flaky deposit found on the anode of one of the experimental diodes. An Ortec nondispersive x-ray analysis unit was used in conjunction with the scanning scope to perform chemical analysis.

B. Materials

The carbonate mix used was Western Electric cathode mix No. 144L. The preparation of the mix is outlined in Table I. The cathode nickel was supplied in the form of a sheet, 0.005 cm in thickness. It was fabricated by the Somers Thin Strip Company from the International Nickel Company's alloy No. 271, melt No. NP13A5HY. The composition of the melt is shown in Table II. All of the gases used with the inlet system were tank gases of industrial purity.

C. Procedure

Filaments were cut from the cathode nickel to form the metal bases of the cathodes. The following procedure was developed for cutting cathodes of uniform width. The nickel sheet was placed in a horizontal position with its edge flush against a vertical surface. A stainless steel single edge razor blade was placed parallel to the vertical surface and the 0.053 cm (21 mil) leaf of a leaf type thickness gauge was inserted between the razor blade and the vertical surface. When the top edge of the razor blade was struck with a hammer a filament was obtained which was 0.061 cm in width within the previously stated limits of error. The experimental diodes were assembled after the filament and anode had been spot welded to the support leads. The diode assembly was rinsed

TABLE I

PROCEDURE FOR PREPARING CATHODE

MIX NO. 144L*

Proportions of Components

Triple Carbonates.....600 g

$BaCO_3$.....49 wt%

$SrCO_3$.....44 wt%

$CaCO_3$..... 7 wt%

Nitrocellulose Solution Diluted.....1800 ml

Amyl Acetate, Grade 2, per ASTM D-318.....960 ml

Particle Size

Mixture was milled until it would pass through a 20 micron sieve.

Impurities

Al	0.001%	Si	0.001%
S	< 0.001%	Cl	< 0.001%

*The cathode mix and accompanying information were generously supplied by the Western Electric Company.

TABLE II

COMPOSITION OF NICKEL ALLOY NO. 271

MELT NP13A5HY*

Component	Mole Percent
Average Active Magnesium	0.51
Aluminum	< 0.005
Carbon	0.09
Cobalt	< 0.001
Columbium and Tantalum	< 0.01
Copper	< 0.01
Iron	< 0.01
Manganese	< 0.01
Silicon	< 0.020
Sulfur	< 0.001
Titanium	< 0.01
Zirconium	< 0.01
BALANCE NICKEL	

*The cathode nickel and accompanying analysis were generously supplied by the Somers Thin Strip Company.

first in PHILLSOLV, a commercial perchlorethylene solvent to remove heavy grease and finger prints, secondly in acetone , and thirdly in methanol. After this procedure, the diode was practically free of residue. The diode, without carbonate coating, was placed in a vacuum of 1.0×10^{-6} Torr or better. Not less than 2.3 A heating current was passed through the filament for approximately 10 minutes. This treatment heated the cathode to an estimated temperature of 750°C and may have removed some chemisorbed impurities. This step was performed as a substitute for the hydrogen or vacuum firing of all tube parts prior to assembly as is commonly done in industry.

The carbonates were mixed with the binder solution by rotation in a jar at 75 rpm for 25 hours or longer. The jar was rotated about its horizontal cylindrical axis. The mixture was applied to the filament with a size No. 1 sable hair brush. Each brush stroke deposited a layer of carbonates on the filament. A few seconds were allowed for drying before the next layer was applied. The final coating thickness was about 0.014 cm. After the diodes had been placed in a dryer at 100°C for 15 minutes they were ready for decomposition and activation. The procedure outlined above was used in preparing all of the experimental diodes except where otherwise noted.

The work progressed in the following manner. First, decomposition of the carbonate coating and activation were studied by analyzing the gaseous products. The ions were

created by the mass spectrometer ion source and were representative of the overall composition within the sample chamber. Spectra taken using ions from the mass spectrometer ion source will be referred to as source spectra. Source spectra were taken while diode emission currents were being drawn also.

Spectra were taken using ions created by the experimental diode once a state of sufficiently high activity was obtained. These will be referred to as diode spectra. Diode spectra were taken at various conditions of gas pressure and composition, cathode temperature, cathode activity, emission current, V_p, and V_{jc}. A bare nickel filament was heated to ascertain whether or not any of the properties of the diode spectrum should be attributed to the heated nickel rather than the diode.

The source spectra taken at high cathode temperature showed that BaO was being evaporated. The scanning electron microscope and nondispersive x-ray analysis unit were used to verify the mass spectrometric evidence of BaO transport as well as to examine the anode deposit.

D. Measurement of the Cathode Temperature

Because of the relationship between cathode temperature and activity a knowledge of the cathode temperature during the experiments was essential to a complete interpretation of the data. Cathode temperatures were reproduced

by measuring and controlling the cathode heating current. The current was measured by a 5 A full scale ac current meter as shown in Figure 4.

When the diode was placed in the sample chamber as shown in Figure 3 the temperature could not be measured with an optical pyrometer since there was no view-port affording a line-of-sight. If a thermocouple had been attached to the cathode in the sample chamber it could have created a short circuit by contacting the shield-can mounted to the J_1 plate. These difficulties were overcome by using a thermocouple to measure the temperature of one cathode in a separate vacuum system with sufficient working space. Figure 5 illustrates the heating current and temperature relationship obtained.

The preceeding relationship is assumed to obtain, within limits of experimental error, for all the experimental cathodes. Deviations were caused by variation in the heat loss due to conduction through the support leads, errors in reading and controlling the heating current, and errors in cutting the cathode filaments. The conduction heat loss was most serious since it caused a sluggishness in reaching an equilibrium temperature when the heating current was changed. A change in heating current resulted in a very rapid approach to equilibrium until the temperature came within about 20°C of the final value. The time required to reach final equilibrium depended upon the total temperature change being made, but was usually five to

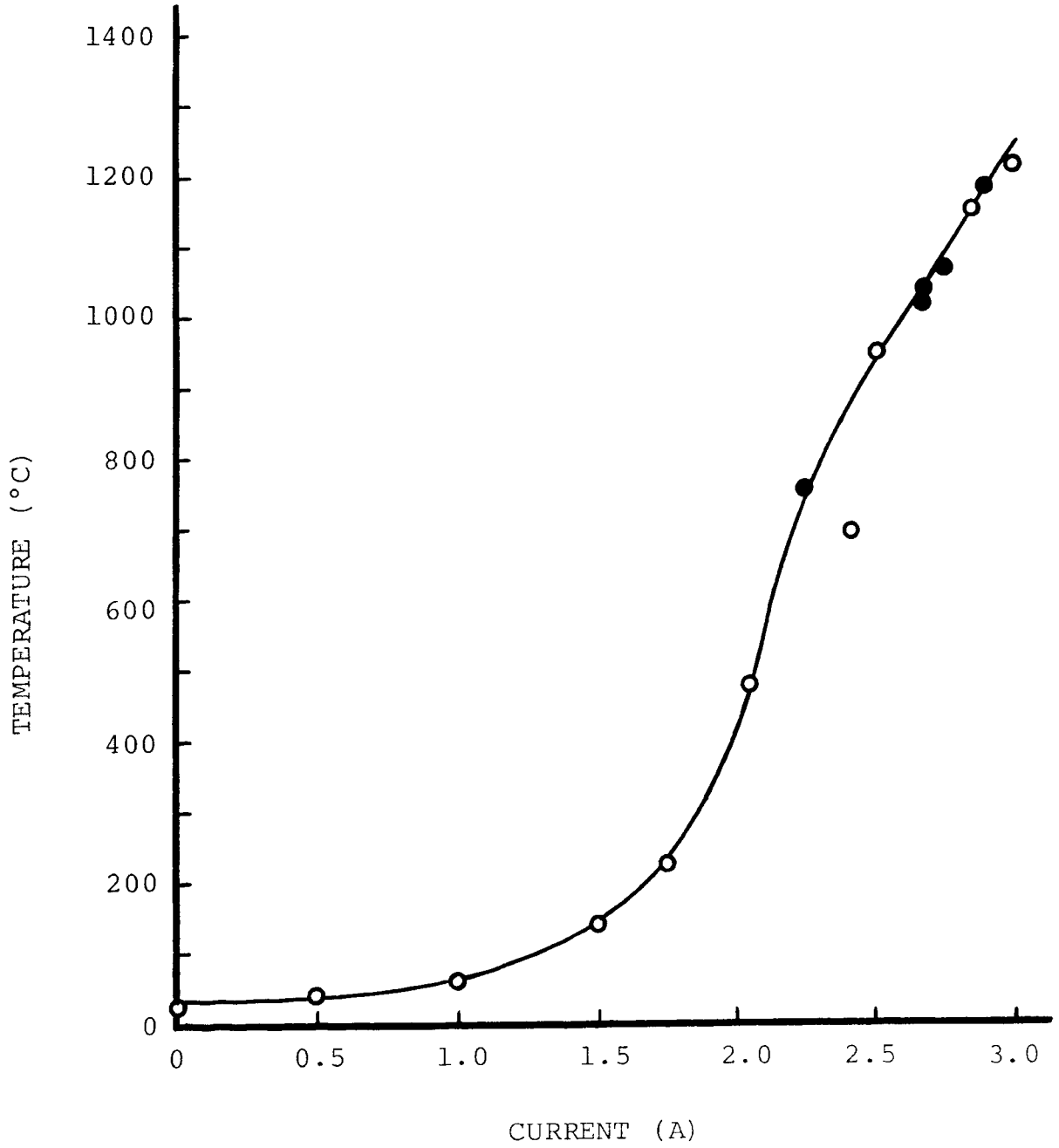

Figure 5. Relationship Between Heating Current and Cathode Temperature

fifteen minutes. It was not always possible to allow sufficient time between measurements or spectra to achieve complete equilibrium. This will be taken into account in discussion of individual experiments in which an error of 30°C or more is suspected.

The thermocouple used in obtaining the relationship shown in Figure 5 was spot welded to the bare filament prior to application of the carbonates. It was Pt-Pt 10% Rd with leg diameters of 0.0025 cm. When a thermocouple is used to determine the temperature of a small object care must be taken to prevent the thermocouple wires from conducting heat away from the sample, thereby changing the temperature to be measured. The ratio of the cross sectional area of the filament to the sum of the cross sectional areas of the thermocouple wires was approximately 30 to 1 in this case. The cooling effect of the thermocouple should have introduced far less error than the lead-loss discussed previously.

In Figure 5, the measurements taken during the initial heat up of the carbonate coated filament were plotted as open circles while those taken during subsequent temperature cycling were plotted as solid circles. The point corresponding to 2.42 A current during the heat up is about 175°C lower than the curve established by the other measurements. This may be partially accounted for by the decomposition of the carbonate coating according to equation

(4). This reaction is endothermic. The heat of reaction at 700°C was calculated to be 62.4 kcal/mole. The part of the energy produced by Joule heating in the filament, above that required to maintain the 700°C temperature, was apparently used by the decomposition reaction.

IV. RESULTS AND DISCUSSION

A. Mass Spectrometric Data

The conditions for bringing an ion beam to focus on the detector are set forth by equation (6a) in Appendix A. Mass spectra were produced by sweeping from low to high values of magnetic field strength (B) in the analyzer section. The data consisted of peaks corresponding to successively higher mass numbers separated by a distance determined by the rate of change of the magnetic field strength and the recorder speed. The relative peak height and changes in relative peak height among spectra were correlated with changes in the experimental variables.

B. Discussion of Results Obtained From the Source Spectra

The decomposition of the carbonates and the spectra of CO_2 were studied through ionization of background gases in the mass spectrometer ion source. The latter clearly illustrates the fragmenting effect the ionizing beam produces in its interaction with the CO_2 molecule. For a more detailed discussion see Appendix F. Source spectra were taken to monitor the composition of the background gas while emission currents were drawn. This was done during the initial stages of emission and at many combinations of V_p and cathode temperature on active cathodes. During these experiments mass spectrometric evidence of BaO

evaporation was obtained. Source spectra were taken while a bare nickel filament was heated in the sample chamber. The results of the preceding studies will be treated following a brief discussion of the properties of the source spectra.

1. Properties of the Source Spectra

A portion of a typical source spectrum is represented by the bar chart in Figure 6. The actual peak shape is shown in the upper right hand corner of the figure. The peaks were symmetrical and narrow because the ions were created within the equipotential region of the source. Mass number to charge ratios (m/q's) were assigned to the prominent peaks by inspection. The prominent peaks were due to C^+, N^+, O^+, OH^+, H_2O^+, CO^+, O_2^+, and CO_2^+ and had m/q's of 12, 14, 16, 17, 18, 28, 32, and 44 respectively.

The spectra exhibited small background peaks at nearly every mass number above mass number 36 and it was possible to assign mass numbers to these peaks by counting the number of peaks between a known peak and the peak in question. The position, x, of the center of each peak was measured along the spectrum base line, arbitrarily taking the center of the peak at m/q of 12 as the origin. A plot of log m/q vs x was found to yield a nearly straight line. The peak positions measured on the spectrum represented in Figure 6 are tabulated in Table III, and the corresponding plot of log m/q vs x is shown in Figure 7. Not

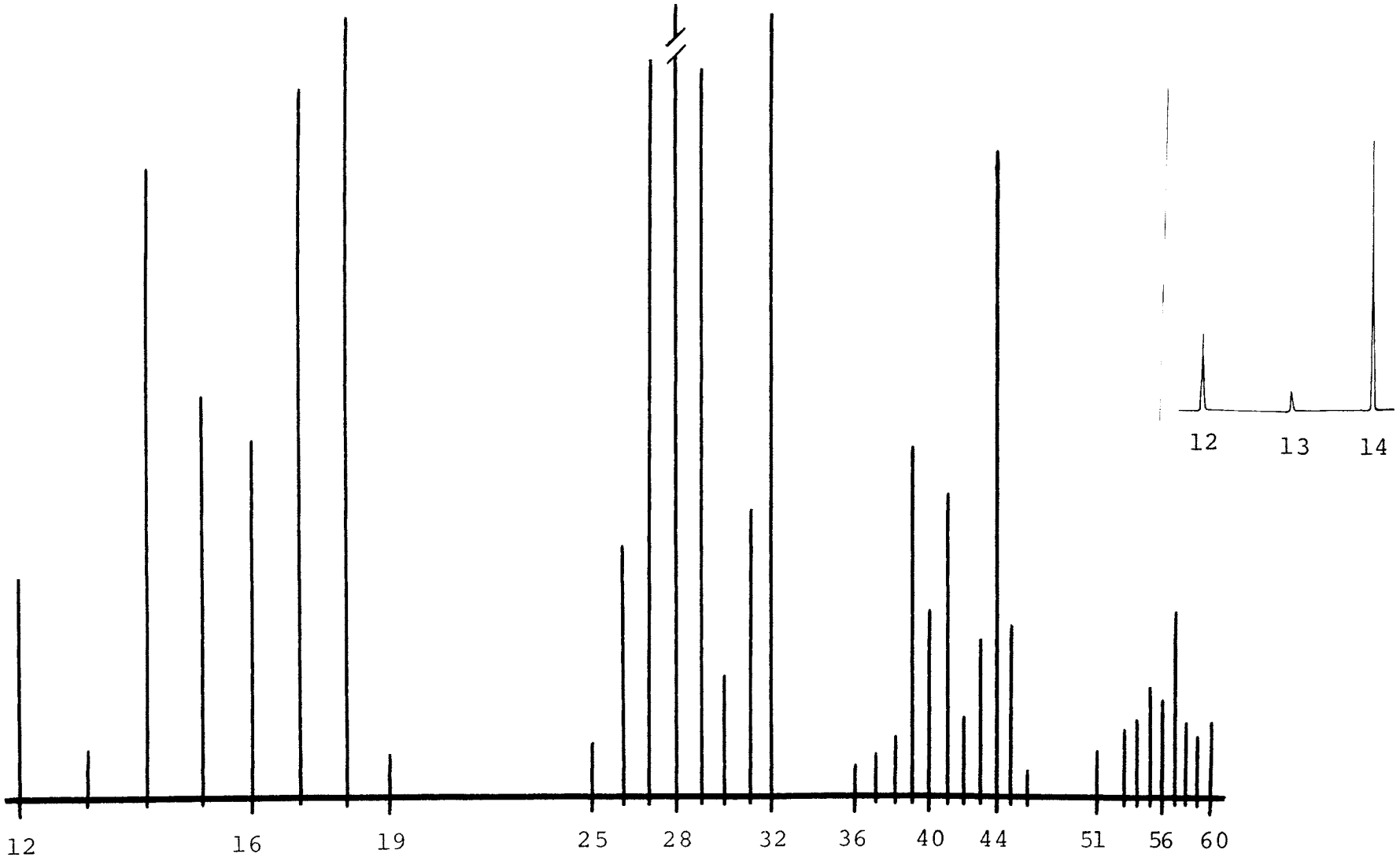

Figure 6. Bar Chart Representation of a Typical Source Spectrum

TABLE III

POSITION OF THE PEAKS IN THE SPECTRUM

ILLUSTRATED IN FIGURE 6

M/Q (amu/e)	X (cm)	M/Q (amu/e)	X (cm)
12*	0.00	38	54.75
13	4.20	39	55.90
14	7.90	40*	56.95
15	11.40	41	58.10
16*	14.50	42	59.15
17	17.50	43	60.20
18	20.30	44*	61.20
19*	23.00	45	62.20
25*	35.80	46	63.15
26	37.65	51*	67.60
27	39.40	53	69.30
28*	41.10	54	70.15
29	42.70	55	70.95
30	44.20	56*	71.75
31	45.65	57	72.55
32*	47.05	58	73.30
36*	52.30	59	74.00
37	53.60	60*	74.75

*Used as a datum point in the plot shown in Figure 7.

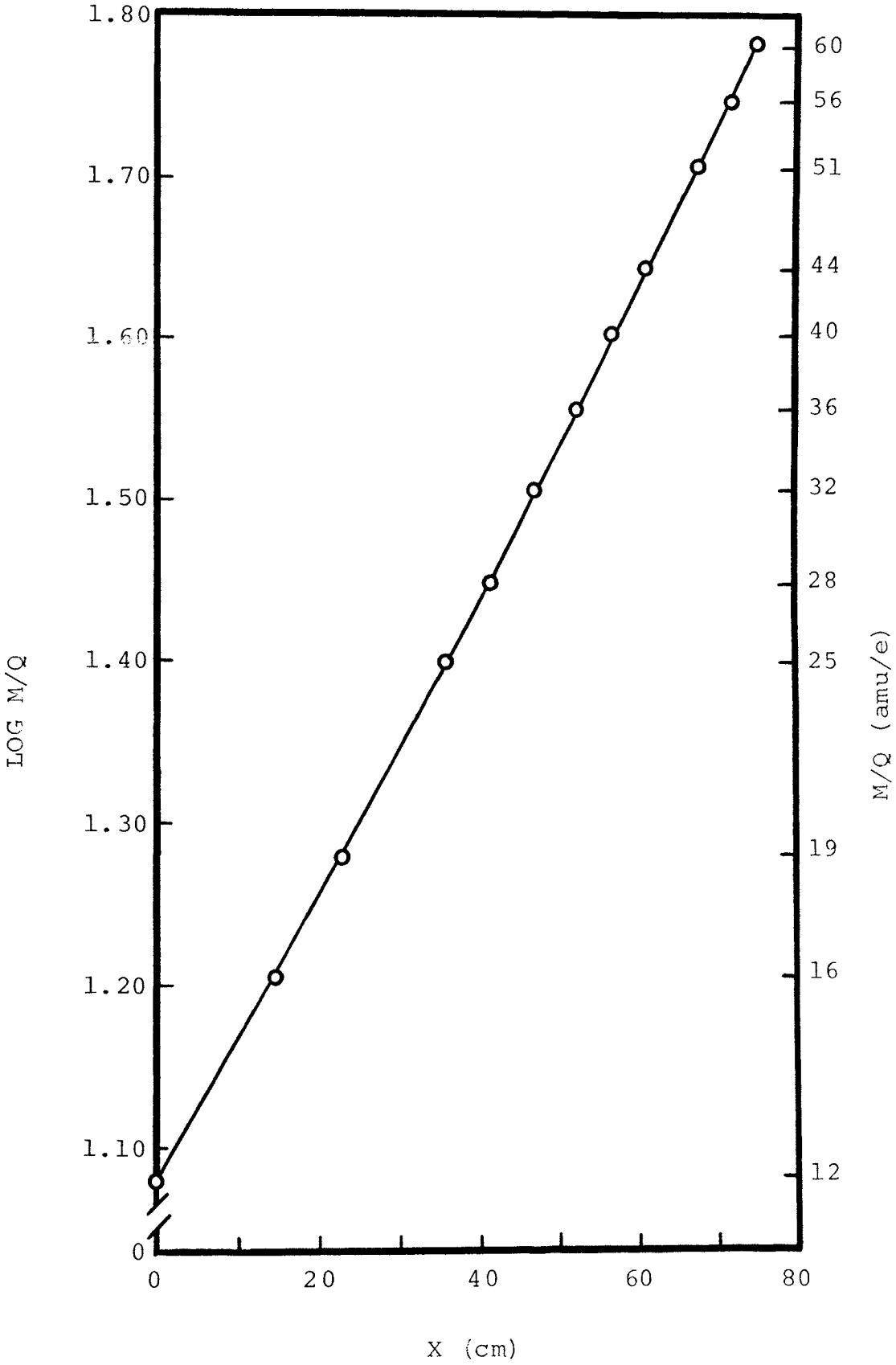

Figure 7. Relationship Between M/Q and X for the Spectrum Illustrated in Figure 6

every peak was plotted in order to avoid crowding at higher mass numbers. Over a small range of mass numbers a linear interpolation or extrapolation was quite accurate in determining the m/q of a peak when the techniques of inspection and counting could not be applied. The accuracy of the linear interpolation was confirmed by interpolation between the peaks at m/q of 28 and m/q of 44 to determine the m/q of the peak at m/q of 32 as if it were unknown. An m/q of 31.99 was obtained as shown by the sample calculation outlining the interpolation procedure in Appendix B.

It is important to consider the following factors when interpreting the information contained in a mass spectrum. First, it is possible for a higher mass number ion to contribute to the peak of a lower mass number ion if it is multicharged. For example, CO^{++} has an m/q of 14 and would contribute to that peak. In addition, there is the possibility of more than one ionic species having the same mass number. This is the case with N_2^+ and CO^+ ions. The fragmenting effect of the ionizing beam can cause one species to contribute to peaks found at m/q's of other species. Fragmentation of the CO_2 molecule is discussed in Appendix F.

2. Decomposition of the Carbonate Coating

The decomposition of the carbonate coating proceeded as outlined below without significant deviation for all

the cathodes used in this research. Some outgassing was observed at a cathode temperature of about 200°C. Source spectra taken at that time showed increases in the relative heights of the peaks at m/q's of 17 and 18. These peaks were attributed to OH^+ and H_2O^+ ions respectively and indicate the release of some adsorbed water vapor. Increasing the temperature led to further outgassing at about 400°C with a second increase in the 17 and 18 peak heights. In addition, the relative height of the peak at m/q of 30 increased by approximately seven fold. The species responsible for this peak could have been NO or CH_4N formed during the decomposition of the binder in the carbonate coating. The peaks at m/q's of 17 and 18 soon decayed to their background value. The peak at m/q of 30 persisted longer and did not return to its background value until the decomposition of the carbonate coating had begun. Its range of appearance corresponded to the temperature range of binder decomposition reported by other investigators.[24,29]

When the cathode heating current was increased to approximately 2.3 A, which corresponded to an equilibrium temperature of 775°C, a large pressure burst was observed. The relative height of the peak at m/q of 44 increased more than twenty fold. The peak at m/q of 28 also increased but to a lesser extent. This corresponds to the beginning of decomposition of the carbonate coating accord-

ing to equation (4). It is likely that the cathode temperature was well below the equilibrium value of 775°C at this time due to the occurrence of the endothermic decomposition reaction. A more precise means of temperature measurement and control would be required in order to determine the lowest temperature at which the decomposition began. A comparison of decompositions revealed the rate of CO_2 evolution and the time required for complete decomposition to be determined by the rate of increase of the heating current. Increases in cathode temperature above 1125°C did not produce enough additional CO_2 to be observed in the source spectra.

The oxide material was removed from one of the cathodes and fresh carbonates were applied. According to Rittner[25] the activating species is depleted in the activation or early in cathode operation. For this reason the "used" filament should have contained a significantly lower concentration of Mg activator than an unused filament. If decomposition of a carbonate on an unused filament yielded more CO (mass number 28) than decomposition on a used filament it would be experimental evidence of the reaction given by equation (6). The data could not be interpreted as evidence of the reaction because the ratios of the mass number 28 peak height to mass number 44 peak height were not the same in both cases when decomposition began, and the rate of increase in cathode heating current was not the same in both cases.

3. The Effect of Drawing an Emission Current

The cathode temperature was held at 1125°C to 1225°C for five to ten minutes after decomposition was completed before V_p was increased from its minimum value of 12.5 V. No emission current could be read on the meter prior to increasing V_p. The smallest meter division was 0.50 mA. Emission currents were increased slowly initially. Later, cathode activity was increased by drawing large currents at high V_p's.

Plumlee and Smith[26] reported an increase in the molecular oxygen peak, m/q of 32, upon drawing low dc emission currents at 800°C; however, this effect was not observed in the present series of experiments. Source spectra were taken while drawing dc current densities on the order of 80 mA/cm^2 at 1125°C to 1225°C. Differences in temperature and current density may account for the fact that molecular oxygen evolution was not observed in this series of experiments, but was observed by Plumlee and Smith. They did not state whether the O_2^+ peak was persistent or only an initial observation.

When high current densities were drawn on an experimental diode for the first time a rise in pressure was observed. Source spectra taken during these pressure increases revealed a nearly uniform rise in peak height, but no significant or consistent changes in relative heights were observed. The peaks at m/q's of 60 and 64 rose in relative height by a very slight amount in a few spectra.

The mass number 64 peak may have been due to sulfur or to a hydrocarbon species. The uniform increase in peak height led to the conclusion that the rise in pressure was due to desorption of gases from the anode by electron bombardment when the current density increased.

C. Discussion of Results Obtained From the Diode Spectra

The diode spectra yielded the most significant results obtained in this research. These included the determination of the origin of the ions bombarding the cathode and their approximate energy at the time of formation. They also furnished evidence of changes in the state of the cathode which were not reflected in the source spectra.

1. Properties of the Diode Spectra

A typical diode spectrum is shown in Figure 8. There are two types of peaks in this spectrum. One type has an asymmetrical distribution showing a build up in height with increasing magnetic field strength. If each dispersed peak is assumed to correspond to ions of a single mass they must have been created with a spread in potential energies. Ions created in the potential gradient between the cathode and anode would have such a spread in energies. The edges of the peaks represent the limits of the spread in energy of the ions; therefore, the edges of the peaks should be related to the cathode and anode potentials.

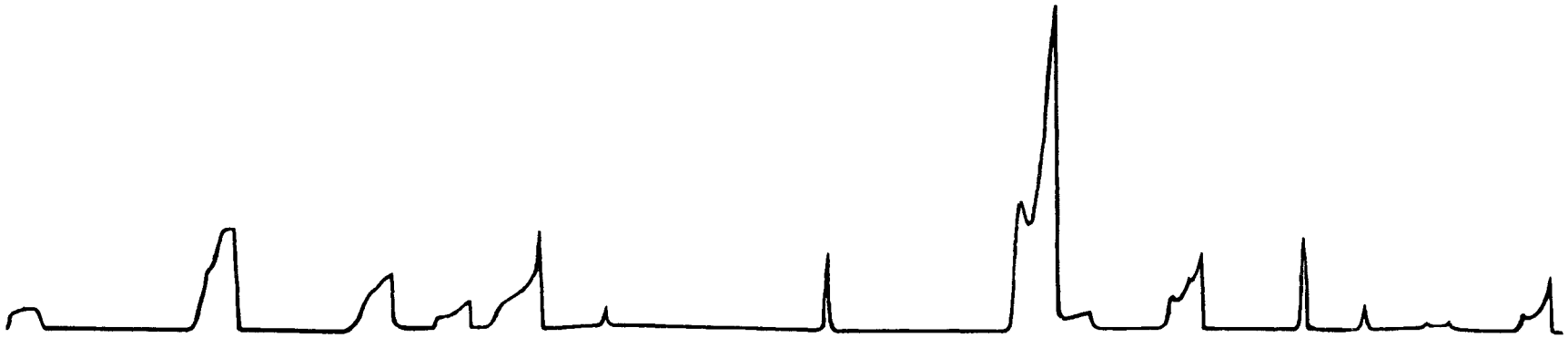

Figure 8. A Typical Diode Spectrum

According to equation (6c) in Appendix A the ions corresponding to the low magnetic field strength edge of the peak were created at a lower voltage than those corresponding to the high field strength edge. This indicates that ions contributing to the left (low field strength) edge of an asymmetrical peak were created in the cathode region while those contributing to the right (high field strength) edge were created in the anode region.

The other type peak observed in the diode spectra was narrow and symmetrical, much like the peaks of the source spectra. This indicated the ions responsible for a spiked peak were created at a uniform potential. The diode consisted of two equipotential surfaces, the cathode and the anode, and the ions responsible for the spikes were in all likelihood created at, or very near, these surfaces. The uncertainty concerning the place of origin of the spiked peaks was eliminated when the procedure for indexing the spectra was developed.

2. Indexing the Diode Spectra

The diode spectra were unfamiliar, and peaks were not observed at every mass number, as illustrated by the spectrum reproduced in Figure 8. Mass numbers could not be assigned by inspection as they had been when the source spectra were indexed. Various gases were admitted into the sample chamber while the diode was in operation to assist in indexing the spectra. Each of these established

the position of one or more of the asymmetrical peaks in the spectra by increasing the relative height of those peaks. CO_2 admission established the position of the peaks with m/q's of 44, 32, 28, 22, 16, and 12. Ar admission established the position of the peaks with m/q's of 40 and 20. The position of the peaks with m/q's of 32 and 16 were further confirmed by the admission of O_2. By superimposing all the known asymmetrical peak positions on a spectrum containing unknown peaks the m/q's of the unknown asymmetrical peaks of m/q less than 44 were determined. The diode spectrum reproduced in Figure 9 will be used as an example during the discussion of the indexing procedure. The m/q's of the asymmetrical peaks as determined through admission of the gases are assigned to their respective peaks in Figure 9. Admitting gases into the sample chamber did not aid in indexing the spike shaped peaks which are lettered a through h.

Since a plot of log m/q vs x was found to yield a nearly straight line for the source spectra this possibility was investigated for the diode spectra. The plot could be made in two ways which differed only in the measurement of the distance x. If x was measured from the origin to the left edges of the asymmetrical peaks the process was called "indexing to the cathode" because the left edges corresponded to ions created in the cathode region. If x was measured from the origin to the right edges of the asymmetrical peaks the process was called "indexing to the anode" because the right edges corresponded to ions created in the anode region. The origin was taken to be the left edge of the asymmetrical

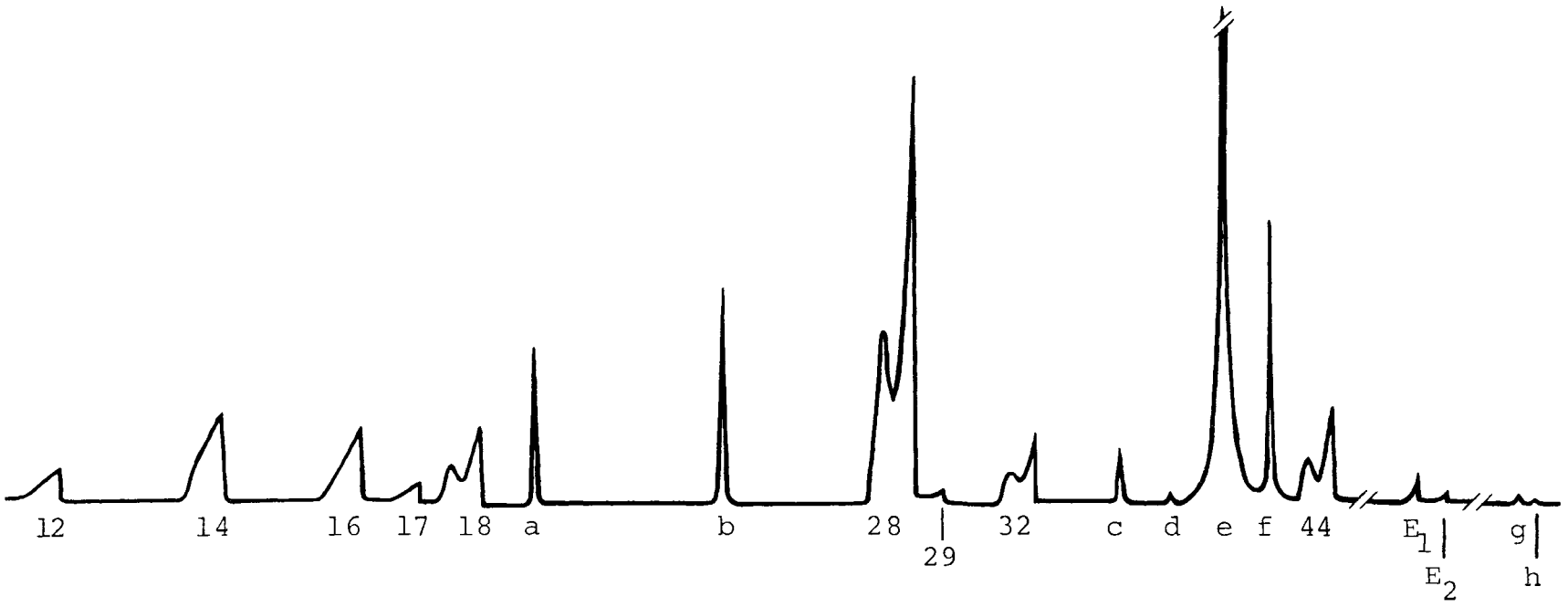

Figure 9. The Diode Spectrum Referred to in the Discussion of the Indexing Procedure

peak at m/q of 12 when indexing to the cathode and the right edge of that peak when indexing to the anode.

The plots of log m/q vs x in Figure 10 and Figure 11 were made using the asymmetrical peaks in Figure 9 to which m/q's have been assigned. Figure 10 is based upon x values measured for indexing to the cathode. These x values and their m/q's are given in Table IV in columns c and d respectively. Figure 11 is based upon x values measured for indexing to the anode. These x values and their m/q's are given in Table IV in columns e and f respectively. A nearly straight line was obtained in Figures 10 and 11. A linear interpolation of log m/q from the measured distance, x, was found to be quite accurate over a small range of mass numbers. The m/q of the peak at mass number 29 was calculated as if it were unknown by interpolation between the peaks at m/q of 28 and 32. An m/q of 28.98 was obtained using the x values measured for indexing to the anode. The interpolation procedure introduced in Appendix B was used.

Once the asymmetrical peaks had been indexed and the accuracy of the interpolation procedure had been established the next step was to interpolate between asymmetrical peaks to determine the m/q's of the spiked peaks. The narrow width and symmetry of the spiked peaks indicated they originated at the cathode or anode surface, but did not lead to a final determination of their origin. For this

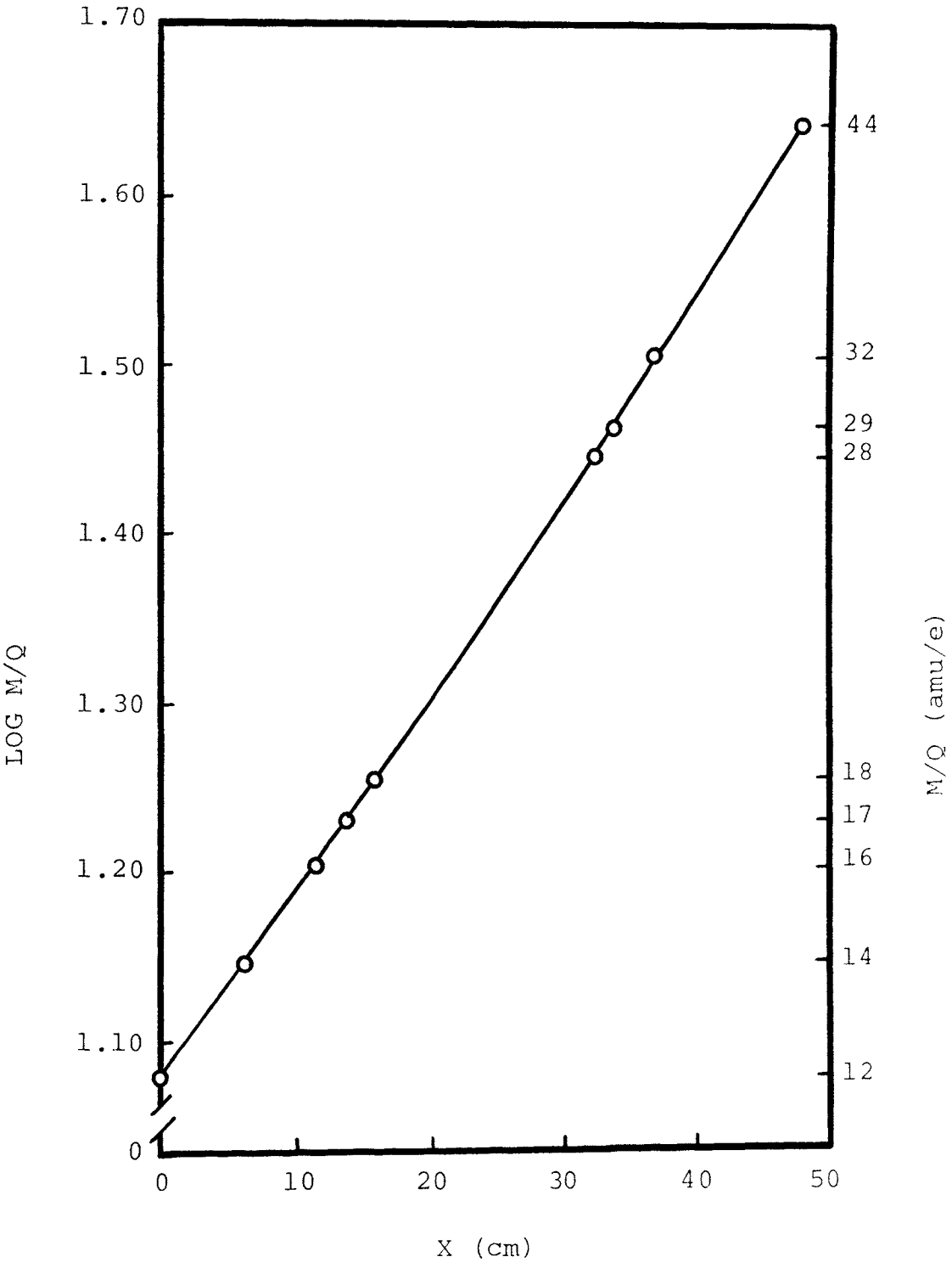

Figure 10. Relationship Between M/Q and X for the Spectrum Illustrated in Figure 9 According to the Scheme of Indexing to the Cathode

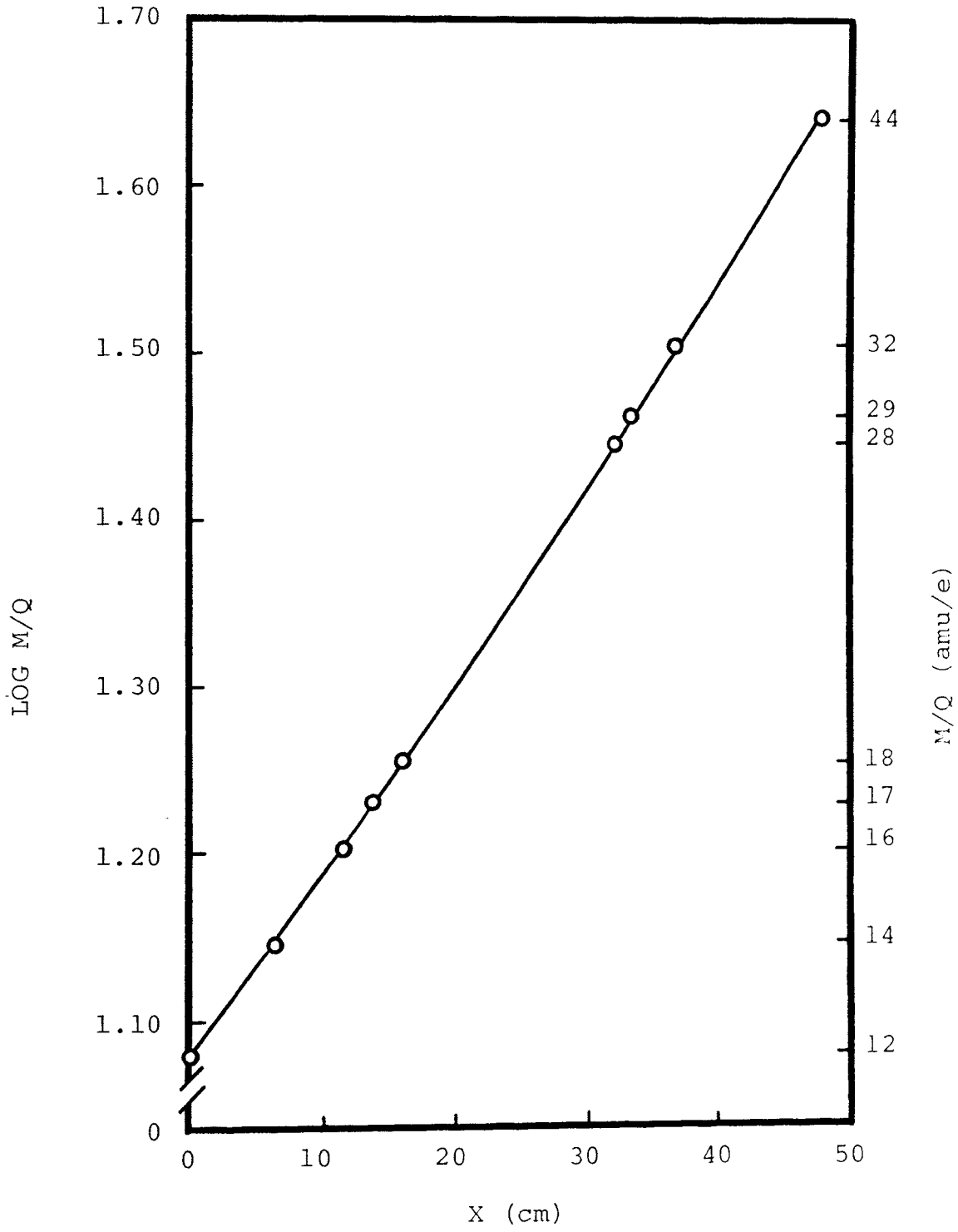

Figure 11. Relationship Between M/Q and X for the Spectrum Illustrated in Figure 9 According to the Scheme of Indexing to the Anode

TABLE IV

SUMMARY OF THE RESULTS OBTAINED BY APPLYING INDEXING PROCEDURES TO THE SPECTRUM ILLUSTRATED IN FIGURE 9

Peak	Peak Type *	Indexing to Cathode		Indexing to Anode		Peaks Used for Inter-polation
		X (cm)	M/Q (amu/e)	X (cm)	M/Q (amu/e)	
a	b	c	d	e	f	g
12	A	0.00	12	0.00	12	
14	A	6.15	14	6.30	14	
16	A	11.53	16	11.45	16	
17	A	13.83	17	13.70	17	
18	A	15.90	18	15.90	18	
a	S	19.55	19.88	17.95	19.02	18 & 28
b	S	26.55	24.06	24.90	22.97	18 & 28
28	A	32.07	28	32.15	28	
29	A	33.77	29	33.35	29	
32	A	36.90	32	36.75	32	
c	S	41.35	36.50	39.80	34.91	32 & 44
d	S	43.30	38.59	41.75	36.92	32 & 44
e	S	45.15	40.69	43.55	38.87	32 & 44
f	S	46.87	42.75	45.30	40.87	32 & 44
44	A	47.95	44	47.84	44	
E_1	A	61.85	65.55	60.64	63.42	
E_2	A	62.95	67.65	61.74	65.45	
g	S	72.05	87.89	70.45	84.01	
h	S	72.85	89.94	71.25	85.96	

*Asymmetrical designated by A, Spiked designated by S

reason the interpolation was made for both schemes of indexing. The position, x, of the spike shaped peaks used in the determination of their m/q's was measured from the origin to the center of the peak. The origin was at the left edge of the asymmetrical peak at m/q of 12 when the interpolation was based upon indexing to the cathode and at the right edge of that peak when the interpolation was based upon indexing to the anode.

Table IV summarizes the results obtained in indexing the spectrum of Figure 9. The measured values of x and the assigned values of m/q for the asymmetrical peaks are listed for each scheme of indexing along with the measured values of x and the calculated values of m/q obtained for the spiked peaks for each scheme of indexing. The peaks are listed in order of occurrence. The asymmetrical peaks which were used in interpolating the m/q of each spiked peak are also listed. The table contrasts the results obtained from the two schemes of indexing. It is apparent that indexing on the cathode leads to nonintegral values of m/q for the spikes between the asymmetrical peaks at m/q's of 32 and 44. Nonintegral peaks can be observed only when doubly or triply charged ions of a higher mass are produced; however, in this case the spectrum beyond m/q of 44 contained only two minor asymmetrical peaks and two very minor spiked peaks. When the spikes of m/q less than 44 were indexed to the anode region the m/q's of all

the peaks were nearly integral. The peak spacing decreases at higher mass numbers and small errors made in measuring x represent a larger percentage error. This partially accounts for the larger deviations from integral values observed for the calculated m/q's between 32 and 44. In addition, the nonlinearity of the relationship between log m/q and x contributed to the error.

The m/q's obtained by indexing to the anode corresponded to known isotope structures. This was convincing evidence that the scheme of indexing the spikes to the anode was correct. If the spikes were assigned the integral values of m/q nearest their calculated value the following were obtained: 19, 23, 35, 37, 39, and 41. The species having an m/q of 19 was assigned to be F^+ which is monoisotopic in nature while those having an m/q of 35 and 37 were assigned to correspond to the two isotopes of Cl^+. The relative abundance of these isotopes of Cl are 75% and 25% respectively,[30] giving a ratio of 3 to 1. The ratio of the peak heights in this spectrum is 2.6 to 1 which was in reasonable agreement with the carefully determined ratio quoted above. The peak at m/q of 23 was assigned to Na^+ which is monoisotopic in nature. The peaks at m/q of 39 and 41 correspond to the two isotopes of K^+. These isotopes occur in abundances of 93% and 7% respectively,[30] giving a ratio of 13.3 to 1. The ratio observed in this spectrum was 10.4 to 1, again, in reasonable agreement with the carefully

determined isotope structure. It is apparent that the spiked peaks should be indexed to the anode and the peaks a, b, c, d, e, and f represent ions of mass 19, 23, 35, 37, 39, and 41 respectively.

The m/q's of the peaks E_1, E_2, g, and h listed below the horizontal line near the bottom of Table IV were calculated by linear extrapolation over a relatively large range of mass numbers. Peaks E_1 and E_2 were calculated to have nonintegral mass numbers according to both schemes of indexing. Peaks g and h were calculated to have m/q's extremely near the integral m/q's of 84 and 86 respectively according to the scheme of indexing to the anode. In view of the occurrence of spike shaped peaks corresponding to the alkali species Na^+ and K^+ it is likely that peaks g and h corresponded to the two natural occurring isotopes of Rb, ^{85}Rb, and ^{87}Rb. The relative abundances of these isotopes are 72.15% and 27.85% respectively.[30] The peaks g and h occur approximately two mass numbers apart as the peaks due to ^{85}Rb and ^{87}Rb would be expected to appear. The ratio of peak heights cannot be compared due to the small absolute heights; however, they do occur in proper order (i.e., the highest peak occurred first). The non-linearity in the log m/q vs x plot is in the direction which would lead to calculated m/q's which are smaller than the actual m/q's when a linear extrapolation is used. The inaccuracy of a linear extrapolation over a large range of mass numbers is thus demonstrated.

3. Discussion of the Spiked Peaks in the Diode Spectra

The species to which the spiked peaks were attributed can be divided into two groups. The halogen group includes F^+ at 19 and Cl^+ at 35 and 37. The alkali group includes Na^+ at 23 and K^+ at 39 and 41. The two groups did not appear to the same degree under all conditions and will be discussed separately.

a. Halogens

The peaks attributed to the halogens were observed over a wide range of operating conditions. They increased in height relative to the asymmetrical peaks as the cathode temperature was increased and as the emission current was increased by increasing V_p at constant temperature. The halogen peaks were initiated at lower current densities than the alkali peaks and drawing a large emission current did not permanently "remove" these species from the spectra. The PHILLSOLV (perchlorethylene) rinse may have been the ultimate source of the halogen peaks.

b. Alkalis

The spikes attributed to the alkali metals were not present in as many spectra as the spikes due to the halogen ions. Their appearance was more effectively initiated by drawing an emission current than by increasing the cathode temperature. The spectrum of Figure 9 was taken

at a time when the amount of alkali emission from the diode was particularly large. The relative intensity of the alkali spikes increased to the proportions shown in Figure 9 when an emission current of 16 mA was obtained at a V_p of 145 V. This represents a current density of 61.5 mA/cm^2 at the cathode surface, and 32 mA/cm^2 at the anode surface. Lower values of the emission current were relatively ineffective at supplying alkali ions at this cathode temperature (1200°C). Halogen ions were, however, supplied by the lower emission currents. The Na^+ peak did appear weakly at a slightly lower value of the emission current.

The appearance of the alkali spikes in Figure 9 was accompanied by an increase in emission current for a constant applied voltage. When V_p was increased to 145 V, the emission current immediately increased to 16.0 mA as stated above; however, it continued to rise to 17.2 mA while V_p remained constant. After a few seconds the emission current decreased to about 16.0 mA. Subsequent spectra did not exhibit alkali peaks as high as those exhibited by the spectrum shown in Figure 9. The increase in emission current at constant V_p is evidence of a change in cathode activity. The correlation between alkali peak appearance and the change in activity suggests that the alkali ions lowered the external work function of the cathode during the period of greater bombardment leading to a more active cathode. The effect may have been transitory due

to the relatively high cathode temperature (1200°C).

The ions responsible for the spike shaped peaks were formed at or very near the anode surface through a combination of heating by radiation and by electron bombardment from the cathode. Source spectra taken under similar conditions did not reveal the release of the alkali or halogen species, but they were plainly seen in the diode spectra.

4. Discussion of the Asymmetrical Peaks in the Diode Spectra

A great deal of information was obtained from an analysis of the width and shape of the asymmetrical peaks. The shape of the peaks was particularly useful in following changes in the state of the cathode.

a. Peak Width

The ions contributing to the left and right edges of the asymmetrical peaks have been shown to originate near the cathode and anode respectively of the experimental diode. The width of the asymmetrical peaks should, therefore, be related to V_p, the potential difference between the cathode and the anode.

Equation (6b) in Appendix A gives the relationship between the magnetic field strength, B, and m/q for ions created at a voltage V. The equation was used to calculate the value of B in Wb/m^2 required to cause the path of an

ion of a given mass number created at the anode potential to be incident upon the detector. This procedure is illustrated using the spectrum reproduced in Figure 9. Table V gives the m/q's of the asymmetrical peaks in Figure 9, the value of B required for detection, and the position of the peak measured according to the scheme of indexing to the anode (i.e., measurements were made to the right edge of the peaks). The voltage used in the calculation of B was the anode potential with respect to ground and it was equal to the sum of V_p, V_{jc}, and the accelerating potential of the ion source. These were equal to 145 V, 95 V, and 2500 V, respectively, and the sum is 2740 V. A sample calculation of the magnetic field strength, B, used to generate column b of Table V is shown in Appendix C.

It was determined that a plot of log B vs x would yield a nearly straight line. This can be inferred from equation (6B) in Appendix A and the fact that a plot of log m/q vs x yields a nearly straight line. Figure 12 illustrates the near linearity of this type of plot for the data in Table V, which was taken from Figure 9. The plot of Figure 12 provides the relationship between the magnetic field strength and the distance along the spectrum base line and allows an interpolation of the value of B corresponding to the left (cathode) edge of an asymmetrical peak. From the value of B thus obtained the voltage (potential) at which the ions corresponding to the left

TABLE V

VALUES OF THE MAGNETIC FIELD STRENGTH, B, CALCULATED TO CORRESPOND TO THE POSITIONS, X, OF THE RIGHT EDGE OF THE ASYMMETRIC PEAKS IN THE SPECTRUM ILLUSTRATED IN FIGURE 9

M/Q (amu/e)	B (Wb/m^2)	X (cm)
a	b	c
12	0.0856	0.00
14	0.0925	6.30
16	0.0988	11.45
17	0.1019	13.70
18	0.1048	15.90
28	0.1307	32.15
29	0.1330	33.35
32	0.1398	36.75
44	0.1639	47.84

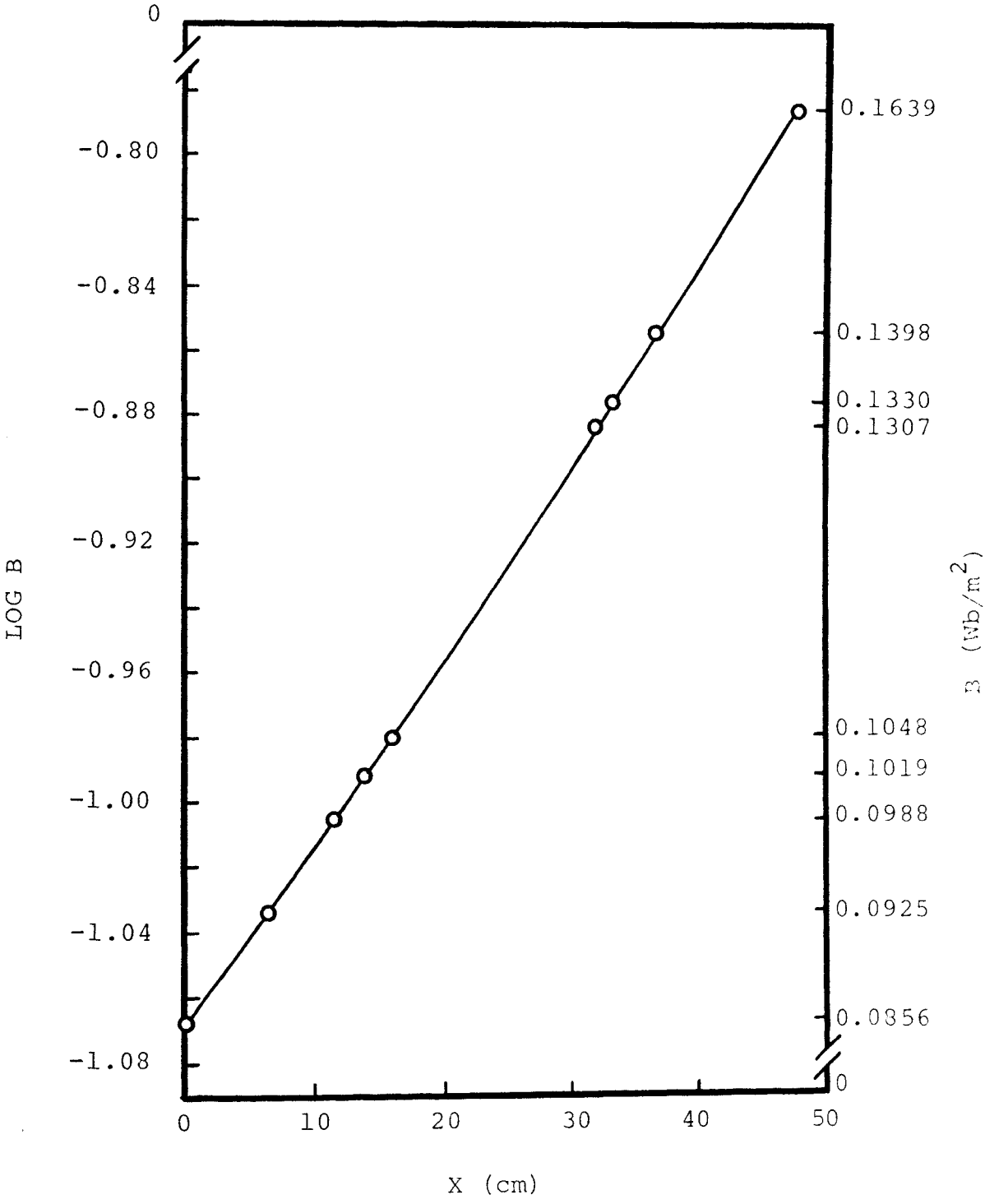

Figure 12. Magnetic Field Strength as a Function of the Distance (X) Along the Base Line for the Spectrum Illustrated in Figure 9

edge of the peak were created can be calculated. This voltage may be compared to the cathode voltage. This procedure provides a quantitative check of the hypothesis that the ions corresponding to the left edge of an asymmetrical peak were created in the cathode region.

A linear interpolation of log B corresponding to the left edge of the peak at m/q of 14 in Figure 9 is shown in the sample calculation in Appendix D. The value of B was found to be 0.0905 Wb/m^2. Using equation (6c) of Appendix A the above value of B was calculated in Appendix E to correspond to a voltage of 2628 V.

The potential of the cathode was the sum of V_{jc} and the accelerating potential, and was equal to 2595 V. The difference of 33 V between the cathode potential and the calculated potential corresponding to the left edge of the peak can be accounted for by considering the energy required to create the ions.

The peak at m/q of 14 was assumed to be N^+; however, nitrogen occurs as the diatomic molecule N_2. The electron energy required to create an N^+ ion from N_2 was found by Hagstrum[31] to equal 24.3 eV. The difference between the cathode potential and the calculated potential corresponding to the left edge of the peak at m/q of 14 should have been 24.3 V rather than 33 V. The remaining discrepancy of 8.7 V is likely due to the uncertainty in determining the left edge of an asymmetrical peak. This error is approximately 6% of the total V_p of 145 V.

b. Peak Shape

The shapes and relative heights of the asymmetrical peaks provided important insights concerning diode operation. The spectra illustrated in Figure 8 and Figure 9 show that the peaks at m/q of 12, 14, 16, and 17 increase in height in a nearly linear way rising to a maximum height at the edge corresponding to the anode region. There were no ions of a single species having an energy greater than the energy of ions created at the anode potential, since the anode was the element at the highest potential in the system. These spectra also show that the asymmetrical peaks at m/q of 18, 28, 32, and 44 possess a somewhat different shape. The most distinguishing characteristic observed for these peaks was the tendency to exhibit two maxima, as shown in Figure 9. The magnitude of this effect was very sensitive to a number of variables, all of which are interrelated.

The relative height of the peak maximum at the edge corresponding to the cathode region was increased in the following ways, and each will be discussed separately:

1. Lowering the cathode temperature
2. Increasing V_p
3. Increasing V_{jc}
4. Admitting CO_2
5. Admitting Ar

1. The Effect of Lowering the Cathode Temperature

When the temperature of a relatively active cathode was lowered from 1060°C to 1000°C the relative height of the peak maximum at the edge corresponding to the cathode region increased. At the same time the emission current dropped from 7.0 mA to 3.0 mA. V_{jc} and V_p were not changed during this experiment. The effect was essentially the same for peaks at m/q's of 18, 28, 32, and 44. The increase in the relative height of the maximum at the left edge upon lowering the cathode temperature is illustrated in Figure 13 for the peak at m/q of 28.

2. The Effect of Increasing V_p

An increase in V_p was accompanied by an increase in the relative height of the peak maximum at the edge corresponding to ions created in the cathode region. This effect was especially pronounced when the increase in V_p yielded little or no further increase in the emission current. The increase observed in the relative height of the maximum at the left edge upon increasing V_p is illustrated in Figure 14 for the peak at m/q of 28. The cathode temperature was 1060°C in both cases. It should be noted that the increase in V_p yielded no additional emission current.

3. The Effect of Increasing V_{jc}

It was discovered that the height of the asymmetrical

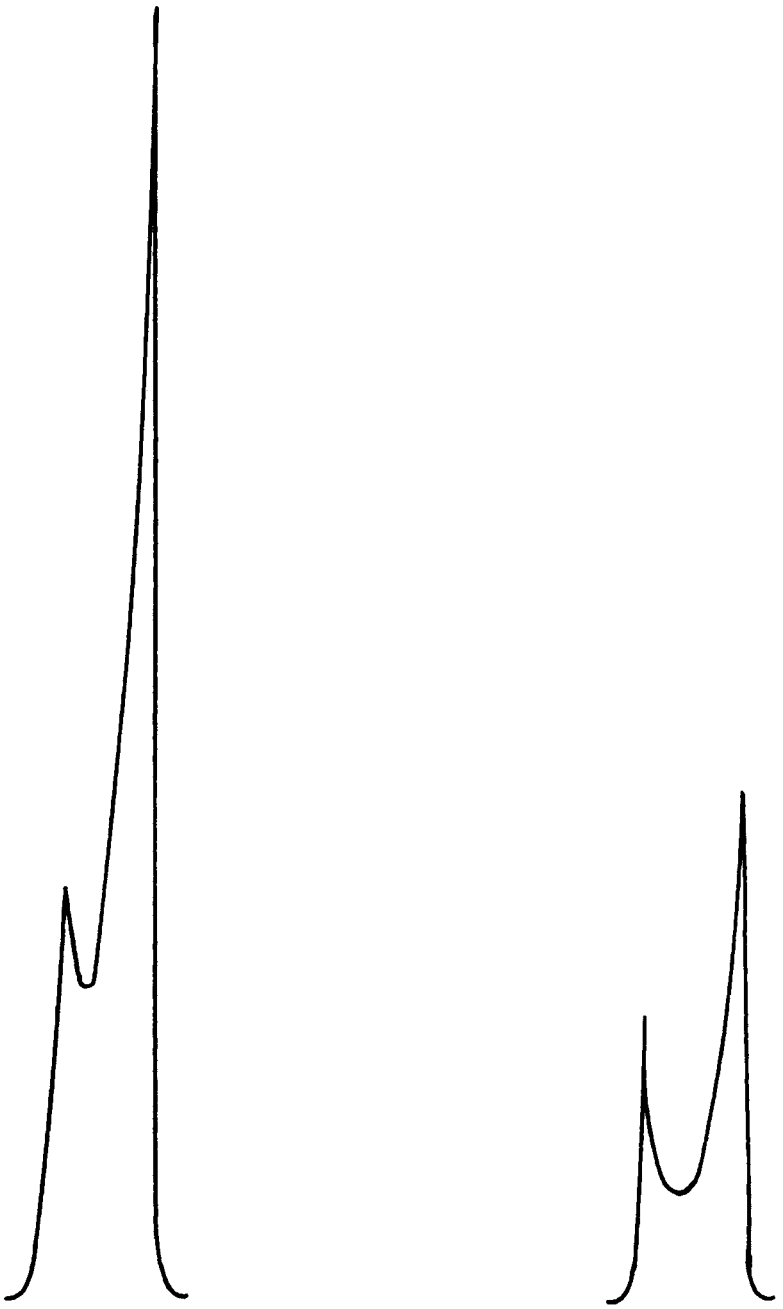

Figure 13. The Effect of Lowering the Cathode Temperature Upon the Shape of the Peak at M/Q of 28

(a)
V_p=105V

(b)
V_p=150V

Figure 14. The Effect of Increasing V_p Upon the Shape of the Peak at M/Q of 28

peaks could be maximized by varying V_{jc}. Setting V_{jc} at 95 V was found to maximize the height of the peak at m/q of 44. The height of the maximum corresponding to ions created in the cathode region increased in relative height over that observed prior to maximizing the mass 44 peak height when the value of V_{jc} was increased from 70 V to 95 V.

4. The Effect of Admitting CO_2

When CO_2 was admitted to a moderately active diode at a cathode temperature of 1190°C the emission current fell from 11 mA to 8 mA at a constant V_p of 130 V. In addition, the admission of CO_2 changed the diode spectrum in the following ways. First, the relative height of the peak at m/q of 44 increased. The value of the ratio of the height of the mass number 44 peak to the height of the mass number 14 peak (I^+_{44}/I^+_{14}) rose from 0.29 to 9.58, an increase of 27.8 fold. The ratio of I^+_{44}/I^+_{14} was chosen as the basis of comparison because the admission of CO_2 did not produce a species contributing to the peak at m/q of 14.

The pressure in the system prior to the admission of CO_2 was 3.9×10^{-7} Torr. The steady state pressure read on the ionization gauge was 7.6×10^{-7} Torr during the CO_2 admission. This demonstrates the importance of allowing the pressure burst due to CO_2 evolution during the decomposition step to completely subside before an emission current

is drawn. A two fold increase in the ionization gauge pressure represents nearly a twenty-eight-fold increase in the relative amount of CO_2^+ ion bombardment of the cathode.

The second way CO_2 admission changed the diode spectrum was to increase the relative height of the peak maximum corresponding to ionization in the cathode region. Figure 15 illustrates this change in peak shape for the peak at m/q of 28. The effect was observed not only for the peaks at m/q of 44, 32, and 28, but also for the peaks at m/q of 17 and 18. Since the admission of CO_2 should not affect the concentration of water vapor to an appreciable extent, the conclusion is that the changes in the shape of the asymmetrical peaks were due to changes in the state of the cathode and not merely an increase in pressure.

5. The Effect of Admitting Ar

When Ar was admitted to a diode of relatively low activity at a cathode temperature of 1190°C and a V_p of 130 V the emission fell from 5.5 mA to 4.5 mA. This was accompanied by an increase in the relative height of the maximum at the low voltage edge of the asymmetrical peaks in the diode spectrum. The effect was observed for the peaks at m/q's of 40 (Ar^+) and 20 (Ar^{++}) and for those at 18, 28, 32, and 44 of the original spectrum. The effect is illustrated in Figure 16 for the peak at m/q of

(a)
Before CO_2 Admission

(b)
After CO_2 Admission

Figure 15. The Effect of CO_2 Admission Upon the Shape of the Peak at M/Q of 28

(a)
Before Ar Admitted

(b)
After Ar Admitted

Figure 16. The Effect of Ar Admission Upon the Shape of the Peak at M/Q of 28

28. The pressure measured by the ionization gauge prior to admission of Ar was 3.7×10^{-7} Torr. The pressure measured by the gauge during Ar admission was 8.0×10^{-7} Torr. The poisoning effect of the Ar^{+} ion bombardment would have likely been greater if the cathode had not been in a state of low activity prior to Ar admission.

The observations discussed above can be unified and related by considering the effect these manipulations have on the state of the cathode. Manipulations 1 and 2 produce the same type of effect in the shape of the asymmetrical peaks in the diode spectrum; however, the first decreased the emission while the second did not decrease emission and in some cases increased it. It is not likely, therefore, that the absolute value of the emission current drawn can be correlated with the increased height of the low voltage edge. Manipulations 1 and 2 do have one common characteristic. Both of these manipulations would decrease the space charge build-up in the region of the cathode. The fact that admission of pure gases such as CO_2 and Ar affected not only the shape of the peaks due to those gases, but affected the shape of other peaks as well is evidence that the state of the cathode was altered in some way. Manipulations 4 and 5 would tend to lower the space charge build-up due to the poisoning effect which these gases produce.

The cathode and anode of the experimental device form an elememtary electrostatic lens. The existence of space

charge in the region near the cathode has an effect similar to the addition of a third element within the lens system. Apparently the focusing of ions of lower energy is much more sensitive to the space charge effect than the ions of higher or intermediate energy. The use of this diode arrangement to study the transition from operation in the space charge region to operation in the Schottky region is a possible extension of this research. The value of the field and current at which the Schottky region begins is often hard to determine strictly from a plot of log j_s vs $\sqrt{V_p}$. When taking data for a Schottky plot it is necessary to use stable cathodes and carefully constructed diodes. Using peak shape in conjunction with Schottky plots would strengthen both techniques.

Another interesting observation regarding the asymmetrical peaks is the fact that the peaks at m/q of 18, 28, 32, and 44 exhibit a strong tendency to take on the shape shown in Figure 13b, 14b, 15b, and 16b, while the peaks at m/q of 12, 14, and 16 do not exhibit this tendency to a great extent. The peaks at m/q of 12 and 16 did exhibit this tendency somewhat when manipulations 2 and 4 were used together. The peaks at m/q of 18, 28, 32, and 44 are due to ions of H_2O^+, CO^+, O_2^+, and CO_2^+ respectively which are subject to fragmentation during collisions with electrons emitted from the experimental diode. The peaks at m/q's of 12, 14, and 16 are due to the monatomic species C^+, N^+, and O^+ respectively and fragmentation is not possible in these

cases.

If a molecule such as CO_2 is struck by an electron and simple ionization takes place then equation (7) describes the process.

$$CO_2(g) + e^- \rightarrow CO_2^+ + 2e^- \qquad (7)$$

If the electron has sufficient energy a process of the type shown in equation (8) may occur.

$$CO_2(g) + e^- \rightarrow CO^+ + \tfrac{1}{2}O_2(g) + 2e^- \qquad (8)$$

If this occurs the CO_2 molecule which could have contributed to the mass number 44 peak is lost to fragmentation. Different types of fragmentation processes produce different species and the energies required vary among processes. The asymmetrical peaks created by the experimental diodes can be thought of as a plot of relative number of ions reaching the detector vs energy at creation. The relative height of the peaks of m/q of 28, 32, and 44 might be lowered at points along the peak distribution corresponding to voltages at which fragmentation occurs. The fragmentation process can not account for variations in the shape of the mass 12, 14, and 16 peaks, and it does not account for the changes in peak shape due to variations in cathode temperature or V_p. The data shows that the peak shape is predominately controlled by the state of the cathode, but does not preclude contributions due to fragmentation.

D. Relative Sensitivity of the Diode and Source Spectra

An area of investigation in which diode spectra proved to be more sensitive than the source spectra was the effect of raising the cathode to a high temperature. In a study of the above type, experimental diodes were introduced into the ionization source of the mass spectrometer and the carbonate decomposition was performed. When the cathode temperature reached 1125°C a small emission current was drawn which was increased to 11 mA. After the cathode had been maintained at 1125°C for more than 34 minutes the cathode temperature was increased to 1160°C. A diode spectrum, taken at 1160°C with V_p equal to 130 V and the emission current equal to 14 mA, yielded an I^+_{44}/I^+_{14} of 1.38. The cathode temperature was lowered to 1000°C while V_p remained at 130 V and the emission current fell to 3.0 mA. The value of I^+_{44}/I^+_{14} fell to 0.666. The cathode temperature was again raised to approximately 1160°C holding V_p constant at 130 V and an emission current of 8.0 mA was obtained. The value of I^+_{44}/I^+_{14} rose to 0.964, indicating the release of CO_2 from the cathode when its temperature was increased. Source spectra taken under similar conditions did not show the release of CO_2.

It is apparent that raising an oxide cathode to a temperature higher than its previous processing temperature results in further outgassing of CO_2 even at these relatively high temperatures. When the processing and operating temper-

atures are lower than the 1100°C to 1200°C temperatures used in this research the amount of CO_2 remaining in the cathode waiting to be released upon an increase in cathode temperature is assumed to be greater. The cathodes used in industry are commonly processed and used at temperatures below 950°C. It is apparent that sudden increases in cathode heating power due to fluctuations in line voltage might result in the release of CO_2 from normal industrial cathodes. The performance of such a tube might be lowered significantly.

The superior sensitivity of the diode spectrum to processes occurring in the diode region is further demonstrated by the occurrence of the alkali and halogen peaks in the diode spectrum. This liberation of alkali and halogen ions was not observed in source spectra taken under similar conditions.

E. Heating a Bare Nickel Filament

A diode was constructed in the same manner and with the same materials used in the previously described experiments; however, the filament was not coated with carbonates. The diode was placed in the mass spectrometer sample chamber and the filament was heated to see if any of the observed properties of the diode spectra should be attributed to the heated nickel rather than emission from the oxide coating. Source spectra taken during the heating

process showed no significant changes as the temperature was increased.

When the filament temperature had been increased to approximately 1125°C the J_1 to filament and anode voltages were set at values used in obtaining diode spectra with oxide coated filaments, and the electron beam in the mass spectrometer ion source was turned off. The bare filament did not emit an electron current large enough to be read on the emission current meter and no diode spectrum was obtained.

While the filament temperature was maintained at 1125°C CO_2 was admitted into the sample chamber. The flow rate was sufficient to raise the pressure measured on the ionization gauge from 4.2×10^{-7} Torr to 7.6×10^{-7} Torr. Source spectra were taken during this time; however, they were curtailed when the source began to operate abnormally. When the source was removed for inspection the ceramic insulators facing the nickel filament of the diode were covered by a metallic film. The shadowing on the insulators indicated that the filament was the source of the film.

The source spectra obtained while the CO_2 was admitted did not reveal the species being transported. Admitting a gas into the sample chamber results in a diminishing of the sensitivity of the mass spectrometer to other constituents. In addition, source spectra obtained during the transport were taken at a low sensitivity setting of the electron multiplier in order to keep the CO_2 peak on scale. For these

reasons the relative peak heights observed in the source spectra indicated only the admission of CO_2. The transport could have been due to nickel atoms evaporating from the filament; however, it did not appear to interfere with the operation of the ion source until CO_2 was admitted. This indicates the CO_2 reacted with the hot filament producing a vapor species containing nickel. The nickel could have been carried by this species to cooler surfaces and deposited as a metallic film. The nickel carbonyl molecule, $Ni(CO)_4$, could have been responsible for the transport; however, the exact mechanism by which the transport occurred was not determined.

At no time during the heating of the bare filament were alkalis observed to be emitted. This is in contrast with the results of Thibault and Secretin[3] and Plumlee and Smith[26] who reported the emission of positive ions of alkali metals commencing at about 500°C. Alkalis could have been emitted in this experiment without being observed. During the initial filament-heat-up, source spectra were taken, but they did not show any increase in relative alkali peak height. This means the filament did not emit a sufficient quantity of alkalis to be reflected in the background composition. When the gradient from the filament to the mass spectrometer ion source was established and the electron beam in the source was turned off the observation of positive ions emitted by the nickel filament would have been possible. No peaks were observed at the tempera-

ture of observation, 1125°C. If positive ions of the alkali metals were emitted by the nickel filament the emission had apparently ceased at this relatively high temperature. This does not preclude low temperature evolution of alkali metal ions present on the nickel filaments as a surface impurity.

The series of experiments described above was successful in showing that the diode spectrum was due to emission from the oxide coating since no diode spectrum was obtained when the coating was omitted. It did not determine the manner in which nickel was transported at 1125°C.

F. Barium Oxide Transport

One cathode was operated for a short period of time at 1370°C. The coated filament failed at this temperature, which was 95% of the absolute melting point of nickel, due to tension applied by the support leads.

The source spectrum taken just prior to failure of the coated filament showed peaks at m/q's of 154, 153, 152, and 151. These peaks correspond to BaO^+ ions in which the mass numbers of the barium isotopes are 138, 137, 136, and 135 respectively. The relative heights of the peaks were consistent with the natural isotopic abundance of barium. A very small peak was observed at m/q of 138, and was assumed to correspond to Ba^+. The failure to observe peaks due to the other isotopes of barium does not invalidate this assumption. The next most frequently occurring isotope,

^{137}Ba, is only one sixth as abundant as ^{138}Ba; therefore, when the ^{138}Ba peak is very weak the others are not observed over background. The Ba^{+} peak could have been produced either by fragmentation of the BaO molecule in the ionizing beam or by thermal dissociation of BaO. There was no indication of the evaporation of SrO or CaO in this spectrum.

A black deposit was found on the anode. When the deposit was examined in the scanning electron microscope nearly spherical globules were found on the surface. Micrographs illustrating this phenomenon are shown in Figure 17. Nondispersive x-ray analysis of the surface showed the presence of Ba and Sr.

A second anode which was never used opposite a filament reaching a temperature higher than 1250°C did not exhibit the black deposit. No globules were observed on the second anode during a similar scanning electron microscope examination. Nondispersive x-ray analysis did, however, show the presence of Ba and Sr.

These observations prove that cathode materials were transported to the anode at high temperatures. Cathode materials may be transported by either an evaporative mechanism or an ion bombardment mechanism. The evaporative mechanism is indicated in the first case since BaO was present in the background gases. The second anode was used during the experiments in which the gases CO_2 and Ar were

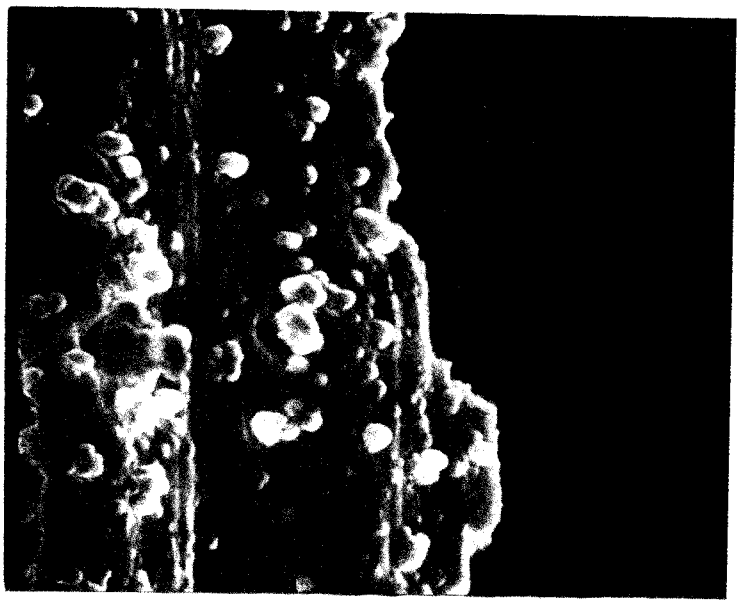

(a)

300x

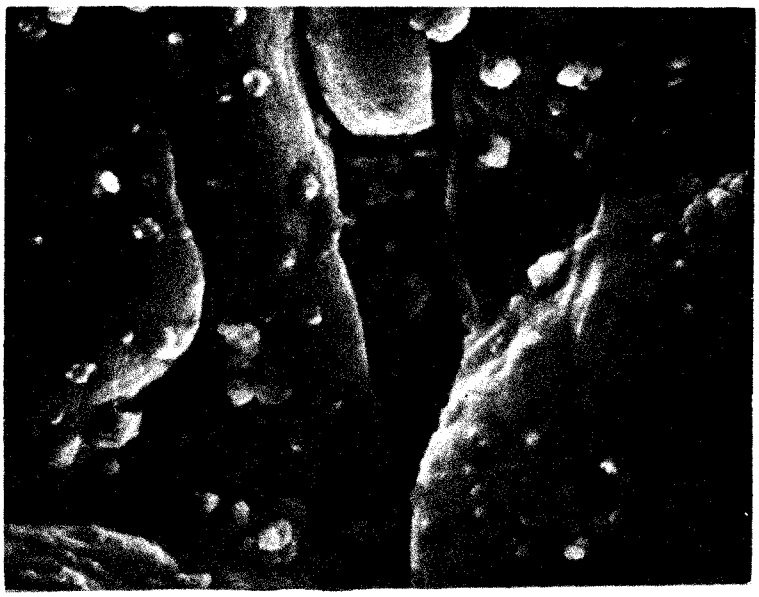

(b)

1000x

Figure 17. Scanning Electron Micrographs of an Anode Which Faced a Cathode Operated at 1370°C

introduced into the system. It was subjected to higher pressures and more severe ion bombardment. Although no globules were detected on this anode, some transport of Ba and Sr did occur. Both the evaporative and the ion bombardment mechanisms may have contributed to the transport in the second case.

G. Summary of Results and Comparison to Those of Other Investigations

The results obtained in the present investigation during the studies of decomposition were quite similar to the results obtained by other investigators. One exception was the appearance of the peak at m/q of 30. The temperature range in which it appeared corresponded to the reported temperature range of binder decomposition,[24,29] and it was attributed to decomposition of the nitrocellulose binder.

The evolution of molecular oxygen from the cathode was not observed when an emission current was drawn as was observed by Plumlee and Smith.[26] The cathode temperature was not the same in the two studies and this may account for the difference in observations.

The diode spectra provided the mass and place of origin of the ions created during diode operation. It was possible to identify ions released at the anode surface by electron bombardment and correlate the width of the asymmetrical peaks with the cathode to anode voltage, V_p. In the present investi-

gation nickel anodes were found to release F^+, Cl^+, Na^+, K^+, and Rb^+ ions, but there was no confirmation of the release of positive ions of oxygen from the anode at cathode temperatures as high as 1200°C and current densities as high as 32 mA/cm^2 at an electron energy of 150 eV.

These results are in qualitative agreement with the results of Young[28] and Plumlee and Smith.[26] It should be noted that the latter investigators studied the effects of electron bombardment of several metals including nickel; however, they reported the release of oxygen was definitely established only for molybdenum anodes.

The diode spectra were found to be more sensitive to processes occurring in the diode region than were the source spectra which reflected changes in the background composition. This is demonstrated by the detection of the release of CO_2 due to cathode outgassing when diode spectra were taken. Source spectra taken during similar increases in cathode temperature did not reveal the evolution of CO_2. The diode spectra were quite adequate for determining the species released from the anode when an emission current was drawn. The identity of the species was not reflected in source spectra taken under similar conditions.

Changes in the state of the cathode were produced by the admission of various gases and by the species released from the anode when an emission current was drawn. The admission of CO_2 and Ar were observed to cause cathode

poisoning which was reflected by an increase in the relative height of the maximum at the left edge of the asymmetrical peaks at m/q's of 18, 28, 32, and 44.

Because the ions contributing to the diode spectra were representative of the ions bombarding the cathode, the effects of positive ion bombardment by specific ions could be correlated with changes in cathode activity. The diode spectrum shown in Figure 9 related an increase in cathode activity to bombardment by alkali ions.

Oxide materials may be transported by evaporation, by positive ion bombardment, or by a combination of these mechanisms. In the present investigation nondispersive x-ray analysis revealed the transport of Ba and Sr at a cathode temperature of 1250°C. At a cathode temperature of 1370°C the presence of BaO vapor was reflected in the source spectrum and spherical globules were observed on the anode surface. Ca was not detected using nondispersive x-ray analysis and neither SrO nor CaO were observed in any source spectra.

V. CONCLUSIONS

The method developed in the present investigation of direct observation of positive ions created during the operation of a simple diode was very sensitive to processes which changed the state of the cathode. The ionic species bombarding the cathode were identified and their region of formation was determined. Changes in the shape of the peaks corresponding to ions created in the interelectrode space were correlated with changes in the amount of space charge existing in the cathode region. A decrease in the amount of space charge led to an increase in the height of the peak maximum which corresponded to ions created in the cathode region.

Alkali and halogen ions were released from the anode when an emission current was drawn. Heavy bombardment of the cathode by alkali ions was associated with an increase in cathode activity. The increase in activity was attributed to a lowering of the external work function by the alkali ions.

Heating an oxide cathode to temperatures as high as, or higher than, previous processing temperatures led to further release of CO_2. This could lead to significant changes in cathode activity in a sealed tube.

At high cathode temperatures (1370°C) BaO was present in the gaseous phase and Ba and Sr were transported to the anode.

VI. FUTURE

Careful decompositions could be performed using filaments of varying activator concentration while monitoring the ratio of the heights of the CO^+ and CO_2^+ peaks in the source spectra. In this way the investigator could search for evidence of the occurrence of the reaction given by equation (6).

A fruitful area of research would be the examination of the diode spectra obtained using anodes of metals other than nickel. For purposes of examining the effects of electron bombardment tungsten filaments could be used rather than oxide cathodes eliminating the need for time consuming decomposition of the oxide coating. Higher cathode temperatures and current densities could also be obtained.

Another promising type of experiment would be a careful determination of the emission current as a function of the plate voltage, V_p, using precision made diodes with smooth, parallel cathode and anode surfaces. The data obtained could be plotted in the form of a Schottky plot such as the one shown in Figure 2. The transition from the space charge region of operation to the Schottky region of operation could be compared to changes in the relative height of the maximum at the left edge of the asymmetrical peaks in the diode spectrum.

In addition, it would be possible to put the anode,

rather than the cathode, next to the mass spectrometer ion source and analyze the spectrum of negative ions emitted by the cathode. A negative, rather than positive, accelerating potential would be required to accomplish the above analysis.

BIBLIOGRAPHY

1. Herrmann, G. and Wagener, S. The Oxide-Coated Cathode Vol. II. London: Chapman and Hall Ltd., 1951.

2. Benjamin, M. and Rooksby, H. P. "Emission from Oxide-Coated Cathodes", Philos. Mag. 15, 810 (January, 1933).

3. Thibault, N. and Secretin, M. "Etude des cathodes a oxydes par spectrometric de masse Analyse des produits gazeux pendant la phase d'activation", Le Vide No. 106, 396 (Juillet-Aout, 1963).

4. Stier, Paul M. "Mass Spectrometric Study of the Activation of Barium Oxide Cathodes", Phys. Rev. 83, 877 (1951).

5. Vick, F. A. and Walley, C. A. "Negative Ion Emission from Oxide-Coated Cathodes", Proc. Phys. Soc. 67B, 169 (1954).

6. Grattidge, W. and Shepherd, A. A. "Negative Ion Emission from Oxide-Coated Cathodes: II", Proc. Phys. Soc. 67B, 177 (1954).

7. Surplice, N. A. "Emission of Negative Ions of Oxygen from Dispenser Cathodes Part 1. Cathodes of Barium Oxide in Sintered Nickel", Brit. J. Appl. Phys. 12, 214 (May, 1961).

8. Arnot, F. L. and Milligan, J. C. "A New Process of Negative Ion Formation", Proc. Roy. Soc. A. 156, 529 (1938).

9. Hollister, H. "Some Effects of Ion Bombardment on the Emitting Properties of Oxide-Coated Cathodes", Cornell University: School of Electrical Engineering. (October, 1960).

10. Koller, Lewis R. "Electron Emission from Oxide Coated Filaments", Phys. Rev. 25, 671 (May, 1925).

11. Herrmann, G. and Wagener, S. The Oxide-Coated Cathode Vol. I. London: Chapman and Hall Ltd., 1951.

12. Nergaard, L. S. "Studies of the Oxide Cathode", RCA Rev. 13, 464 (1952).

13. Becker, J. A. "Phenomena in Oxide Coated Filaments", Phys. Rev. 34, 1323 (November, 1929).

14. Prescott, C. H. Jr., and Morrison, James. "The Oxide-Coated Filament. The Relation Between Thermionic Emission and the Content of Free Alkaline-Earth Metal", J. Amer. Chem. Soc. 60, 3047 (1938).

15. Dushman, S. "Thermionic Emission", Reviews of Modern Physics 2, 381 (October, 1930).

16. Weast, R. C. (ed.). Handbook of Chemistry and Physics. Cleveland: The Chemical Rubber Company, 1969-70.

17. De Vore, Henry B. "Photoconductivity Study of Activation of Barium Oxide", RCA Rev. 13, 453 (December, 1952).

18. Thomas, D. G., Hannay N. B. (ed.). Semiconductors. New York: Reinhold, 1959.

19. Krumhansl, J. A. "Energy Levels in BaO", Phys. Rev. 82, 573 (May 1951).

20. Pell, E. M. "The Hall Effect in Single Crystals of Barium Oxide", Phys. Rev. 87, 457 (August, 1952).

21. Wright, Ralph and Skutt, H. Electronics: Circuits and Devices. New York: Ronald Press Company, 1965.

22. Eisenstein, Albert S. Advances in Electronics. New York: Academic Press Inc., 1948.

23. Jenkins, R. O. and Trodden, W. G. Electron and Ion Emission from Solids. New York: Dover Publications, Inc., 1965.

24. Rosebury, Fred. Handbook of Electron Tube and Vacuum Techniques. Reading: Addison-Wesley, 1965.

25. Rittner, Edmund S. "A Theoretical Study of the Chemistry of the Oxide Cathode", Philips Res. Rep. 8, 184 (1953).

26. Plumlee, R. H. and Smith, L. P. "Mass Spectrometric Study of Solids I. Preliminary Study of Sublimation Characteristics of Oxide Cathode Materials", J. Appl. Phys. 21, 811 (August, 1950).

27. Hamaker, H. C., Bruining, H., and Aten, A. H. W., Jr. "On the Activation of Oxide-Coated Cathodes", Philips Res. Rep. 2, 171 (1947).

28. Young, J. R. "Evolution of Gases and Ions from Different Anodes Under Electron Bombardment", J. Appl. Phys. 31, 921 (May, 1960).

29. Kohl, Walter H. Handbook of Materials and Techniques for Vacuum Diodes. New York: Reinhold Publishing Company, 1967.

30. Holden, N. E. and Walker, F. M. "Chart of the Nuclides", Knolls Atomic Power Laboratory, General Electric Company, 10th Edition, 1968.

31. Hagstrum, Homer D. "Ionization by Electron Impact in CO, N_2, NO, and O_2", Reviews of Modern Physics 23, 185 (July, 1951).

32. Instruction Manual 12"-90°HT Mass Spectrometer Nuclide Corporation, State College, Pennsylvania, 1965.

VITA

Larry Alton Addington was born on August 25, 1947, in Neosho, Missouri. He received his elementary education in Elwood, Kansas, and his secondary education in Hermitage, Missouri. He received a Bachelor of Science degree in Ceramic Engineering from the University of Missouri-Rolla in January of 1970, and was commissioned a Second Lieutenant in the United State Army Reserve at that time.

He has been enrolled in the Graduate School of the University of Missouri-Rolla since February 1970. He held a Materials Research stipend from February 1970 to August 1970. He has been the recipient of a National Science Foundation Traineeship from September 1970 to August 1971.

He was married to the former Miss Janet Marie Oesch of Weaubleau, Missouri, in December 1968.

APPENDICES

APPENDIX A

FOCUSING CONDITIONS FOR THE MASS SPECTROMETER[32]

When a charged particle moving at constant velocity enters a uniform magnetic field moving in a direction perpendicular to the direction of the magnetic field it will travel in a circular path. The force exerted on the particle by the magnetic field (qvB) is the centripetal force ($\frac{mv^2}{R}$) holding the particle in the circular path. Equating these leads to:

$$\frac{mv^2}{R} = qvB \qquad (1)$$

where: m = mass of the particle in kg

v = velocity of the particle in m/sec

R = radius of path in m

q = charge on the particle in C

B = magnetic field strength in Wb/m^2

Solving equation (1) for v:

$$v = \frac{BqR}{m} \qquad (2)$$

The velocity at which the particle enters the magnetic field is given by its kinetic energy ($\frac{1}{2}mv^2$) which is equal to the charge times the potential through which it was accelerated.

$$\text{Kinetic Energy} = \tfrac{1}{2}mv^2 = qV \qquad (3)$$

Solving once again for v:

$$v = \sqrt{\frac{2qV}{m}} \qquad (4)$$

where: V = potential at which ion was formed in V.

Equating (2) and (4):

$$\frac{BqR}{m} = \sqrt{\frac{2qV}{m}} \qquad (5)$$

Equation (5) can be solved for the mass to charge ratio, m/q, the magnetic field strength, B, or the potential of ion formation, V:

$$\frac{m}{q} = \frac{R^2B^2}{2V} \qquad (6a)$$

$$B = \sqrt{(\frac{m}{q})\frac{2V}{R^2}} \qquad (6b)$$

$$V = \frac{R^2B^2}{2(\frac{m}{q})} \qquad (6c)$$

APPENDIX B

LINEAR INTERPOLATION OF LOG M/Q FROM PEAK POSITION, X

m/q may be expressed in amu/e rather than kg/C

m/q	log m/q	X (cm; TABLE IV)
28	1.447	41.10
unkn	log m/q) unkn	47.05
44	1.643	61.20

$$\log\ m/q)\,unkn = 1.447 + (1.643-1.447)\left(\frac{47.05-41.10}{61.20-41.10}\right)$$

$$\log\ m/q)\,unkn = 1.505$$

$$m/q)\,unkn = 31.99$$

APPENDIX C

CALCULATION OF B FROM M/Q AND V

Using equation (6b) of Appendix A:

$$B = \sqrt{\left(\frac{m}{q}\right)\frac{2V}{R^2}}$$

where: $R = 12 \text{ in.} \left(\frac{1 \quad m}{39.4 \text{ in.}}\right) = 3.046 \times 10^{-1} \text{ m}$

This sample calculation will be based upon the peak at m/q = 14 amu/e. The ions were formed at a potential of 2740 V. M/Q must be converted to kg/C.

$$\frac{m}{q} = 14 \frac{\text{amu}}{e} \left(\frac{1.66\text{x}10^{-27}\text{kg}}{\text{amu}}\right) \left(\frac{1e}{1.602\text{x}10^{-19}\text{C}}\right)$$

$$= 14.51 \times 10^{-8} \frac{\text{kg}}{\text{C}}$$

$$B)_{14} = \sqrt{(14.51\text{x}10^{-8} \frac{\text{kg}}{\text{C}}) \left[\frac{2(2740\text{V})}{(3.046\text{x}10^{-1}\text{m})^2}\right]}$$

$$= 0.0925 \frac{\text{Wb}}{\text{m}^2}$$

APPENDIX D

LINEAR INTERPOLATION OF LOG B CORRESPONDING TO LEFT EDGE OF AN ASYMMETRICAL PEAK FROM X

In this sample calculation the magnetic field strength, B, corresponding to the left edge of the peak at m/q of 14 will be interpolated between the known B values at the right edges of the peaks at m/q of 12 and 14 in Figure 9.

B (Known values from TABLE V; Wb/m^2)	log B	X (Measured from right edge of peak at m/q of 12; cm)
$B)_{12}^{right} = 0.0856$	-1.068	0.00
$B)_{14}^{left} =$ unkn	unkn	4.60
$B)_{14}^{right} = 0.0925$	-1.034	6.30

$$\log B)_{14}^{left} = -1.068 + [-1.034 - (-1.068)] \frac{4.60-0.00}{6.30-0.00}$$

$$\log B)_{14}^{left} = -1.0432$$

$$B)_{14}^{left} = 0.0905$$

APPENDIX E

CALCULATION OF V CORRESPONDING TO THE LEFT EDGE OF AN ASYMMETRICAL PEAK FROM THE CORRESPONDING VALUE OF B

This sample calculation will be performed using the value of B corresponding to the left edge of the peak at m/q of 14 in Figure 9 as determined in Appendix D.

Using equation (6c) in Appendix A:

$$V = \frac{R^2 B^2}{2(\frac{m}{q})}$$

$$V)_{14}^{\text{left}} = \frac{(3.046 \times 10^{-1}\,\text{m})^2 (0.0905 \frac{\text{Wb}}{\text{m}^2})^2}{2(14.51 \times 10^{-8}\ \frac{\text{kg}}{\text{C}})}$$

$$V)_{14}^{\text{left}} = 2628\ \text{V}$$

APPENDIX F

THE SPECTRUM OF CARBON DIOXIDE

Tank CO_2 was admitted into the sample chamber of the mass spectrometer at a flow rate which raised the pressure measured on the ionization gauge from 4.5×10^{-7} Torr to 7.0×10^{-6} Torr. The latter pressure is within the range of pressures produced during the decomposition of the carbonates.

Source spectra were taken while the energy of the electrons in the ionizing beam was increased from 20 eV to 100 eV in increments of 10 eV. The heights of the peaks corresponding to the fragmentation products of CO_2 were measured, and the ratio of each of these peak heights to the CO_2^+ peak height was calculated at each value of the electron voltage. The fragmentation products of CO_2 are CO^+, O_2^+, O^+, and C^+. These appear at m/q's of 28, 32, 16, and 12 respectively. CO_2^{++} is also formed and appears at an m/q of 22. The amount of energy required to form a fragment is dependent upon bond strength; therefore, all fragments are not produced at low electron energies. The C^+ fragment was not observed until the electron voltage reached 30 eV. The CO_2^{++} ion was not observed until the electron energy reached 50 eV. These values are not necessarily the lowest energies at which the species can be formed, but they are the lowest values for which the species were observed in this experiment.

The way in which the relative peak height of the products of CO_2 fragmentation varied with electron energy is shown in Figure 18. The figure indicates that electrons having an energy of 80 eV appear to be particularly effective in fragmenting the CO_2 molecule. The data may be misleading since the ionizing electron current was not constant as the electron voltage was increased. The ionizing electron current was three to four times larger at 80 eV than it had been at previous electron energies; therefore, more ions were created and the signal received by the electron multiplier was stronger. The strip chart recorder was used in obtaining the data shown in Figure 18. When this recorder receives a strong signal over a short time span the pen is unable to follow the signal as closely as it could for a weaker signal, and the recorded peak height is less than it should have been. The ratios shown in Figure 18 were all taken relative to the CO_2^+ peak height, and a recorder induced error in measuring the height of the CO_2^+ peak would lead to higher calculated ratios than actually existed. This is the most probable explanation of the apparent efficiency of 80 eV electrons in fragmenting the CO_2 molecule.

This experiment demonstrates the fragmenting effect of the ionizing electron beam. It also shows the importance of using a recorder that is able to follow the signal accurately if relative heights are to be used quantitatively.

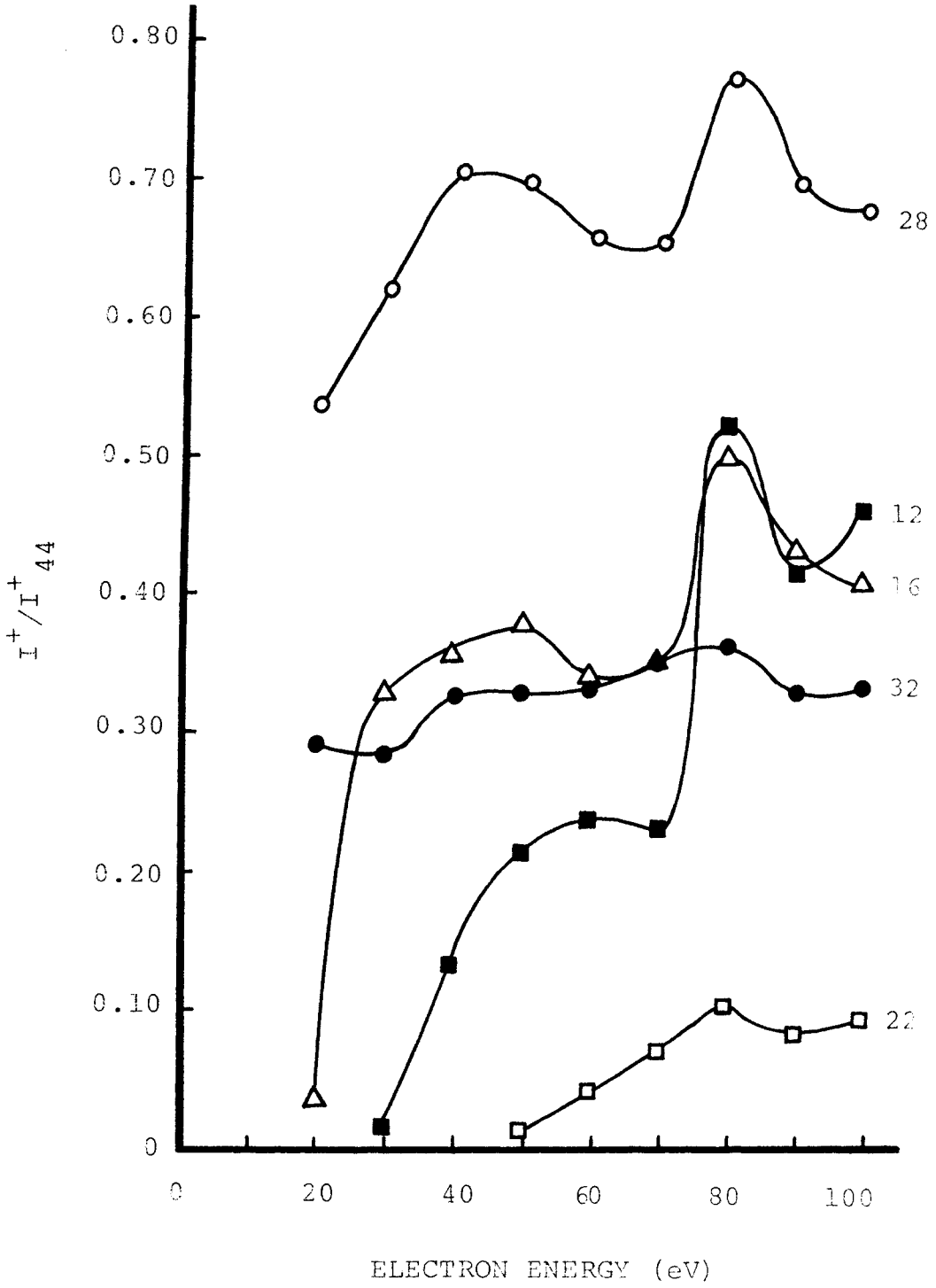

Figure 18. The Relative Heights of the Peaks Due to CO_2 Fragmentation as a Function of Ionizing Electron Voltage

In subsequent experiments the oscillograph recorder was used and the interpretation of the data obtained in other experiments was not jeopardized by this type of error.